

# JGR Biogeosciences

## RESEARCH ARTICLE

10.1029/2021JG006281

### Key Points:

- Most throughfall event dissolved organic carbon (DOC) fluxes were ~10–100 times larger than stream fluxes, but the imbalance narrowed for larger storms (>30 mm)
- Approximately 2–5 times more DOC and total dissolved nitrogen (TDN) was removed from trees than exported from the catchment in streams annually
- The influence of event size on tree and stream fluxes has important implications for forested ecosystems experiencing climate change

### Supporting Information:

Supporting Information may be found in the online version of this article.

### Correspondence to:

K. A. Ryan,  
ryan.kevi@northeastern.edu

### Citation:

Ryan, K. A., Adler, T., Chalmers, A., Perdrial, J., Shanley, J. B., & Stubbins, A. (2021). Event scale relationships of DOC and TDN fluxes in throughfall and stemflow diverge from stream exports in a forested catchment. *Journal of Geophysical Research: Biogeosciences*, 126, e2021JG006281. <https://doi.org/10.1029/2021JG006281>

Received 5 FEB 2021  
Accepted 6 JUL 2021

### Author Contributions:

**Conceptualization:** Kevin A. Ryan, Ann Chalmers, Julia Perdrial, James B. Shanley, Aron Stubbins  
**Data curation:** Kevin A. Ryan  
**Formal analysis:** Kevin A. Ryan  
**Funding acquisition:** Kevin A. Ryan, James B. Shanley, Aron Stubbins  
**Investigation:** Kevin A. Ryan, Thomas Adler, Ann Chalmers, Julia Perdrial, James B. Shanley, Aron Stubbins  
**Methodology:** Kevin A. Ryan, Thomas Adler, Ann Chalmers, Julia Perdrial, James B. Shanley, Aron Stubbins  
**Project Administration:** Kevin A. Ryan

© 2021. American Geophysical Union.  
All Rights Reserved.

## Event Scale Relationships of DOC and TDN Fluxes in Throughfall and Stemflow Diverge From Stream Exports in a Forested Catchment

Kevin A. Ryan<sup>1</sup> , Thomas Adler<sup>2</sup>, Ann Chalmers<sup>3</sup>, Julia Perdrial<sup>2</sup> , James B. Shanley<sup>3</sup>, and Aron Stubbins<sup>1,4</sup> 

<sup>1</sup>Department of Marine and Environmental Sciences, Northeastern University, Boston, MA, USA, <sup>2</sup>University of Vermont, Burlington, VT, USA, <sup>3</sup>U.S. Geological Survey, Montpelier, VT, USA, <sup>4</sup>Departments of Chemistry and Chemical Biology and Civil and Environmental Engineering, Northeastern University, Boston, MA, USA

**Abstract** Aquatic fluxes of carbon and nutrients link terrestrial and aquatic ecosystems. Within forests, storm events drive both the delivery of carbon and nitrogen to the forest floor and the export of these solutes from the land via streams. To increase understanding of the relationships between hydrologic event character and the relative fluxes of carbon and nitrogen in throughfall, stemflow and streams, we measured dissolved organic carbon (DOC) and total dissolved nitrogen (TDN) concentrations in each flow path for 23 events in a forested watershed in Vermont, USA. DOC and TDN concentrations increased with streamflow, indicating their export was limited by water transport of catchment stores. DOC and TDN concentrations in throughfall and stemflow decreased exponentially with increasing precipitation, suggesting that precipitation removed a portion of available sources from tree surfaces during the events. DOC and TDN fluxes were estimated for 76 events across a 2-year period. For most events, throughfall and stemflow fluxes greatly exceeded stream fluxes, but the imbalance narrowed for larger storms (>30 mm). The largest 10 stream events exported 40% of all stream event DOC whereas those same 10 events contributed 14% of all throughfall export. Approximately 2–5 times more DOC and TDN was exported from trees during rain events than left the catchment via streams annually. The diverging influence of event size on tree versus stream fluxes has important implications for forested ecosystems as hydrological events increase in intensity and frequency due to climate change.

**Plain Language Summary** Rainfall over forests links carbon and nutrients on tree surfaces to the forest floor and streams. Rain falling through the canopy is called throughfall while water running down the tree trunk is called stemflow. The ultimate fate of throughfall and stemflow is uncertain. We measured carbon and nitrogen dissolved in throughfall, stemflow, and stream water during rain events in Vermont. We then used rain event size to estimate how much carbon and nitrogen were transported by throughfall and stemflow during a 2-year period, which we then compared with the amount of carbon and nitrogen leaving the forest in streams. The results indicated that the carbon and nitrogen in throughfall and stemflow were washed from tree surfaces and diluted by bigger storms whereas carbon and nitrogen in the streams became more concentrated. Climate change could alter the amount of carbon and nutrients in the forest that is carried away by water by changing the frequency and timing of small and large storms occurring throughout the year.

## 1. Introduction

Estimating the transfer of terrigenous carbon and nutrients to aquatic systems remains a fundamental challenge for carbon cycle and ecosystem studies (Drake et al., 2018; Webster & Meyer, 1997). In order to predict how terrestrial and aquatic carbon budgets will respond to climate and land use change, an understanding of the processes controlling land and inland water carbon cycling is required (Tank et al., 2018). The first interactions between terrestrial carbon sources and water inputs to forested ecosystems occur within the tree canopy, which partitions precipitation into throughfall and stemflow. Throughfall is precipitation that falls on and through the canopy to the forest floor and typically comprises the largest fraction of incident precipitation (Levia & Frost, 2006). Stemflow is precipitation that flows along tree surfaces to the base of tree trunks and typically accounts for a lower percentage of total rainfall (<10%) in forests globally (Levia

**Resources:** Kevin A. Ryan, Ann Chalmers, Julia Perdrial, James B. Shanley, Aron Stubbins

**Software:** Kevin A. Ryan

**Supervision:** Kevin A. Ryan, Ann Chalmers, Julia Perdrial, James B. Shanley, Aron Stubbins

**Validation:** Kevin A. Ryan

**Visualization:** Kevin A. Ryan, James B. Shanley, Aron Stubbins

**Writing – original draft:** Kevin A. Ryan

**Writing – review & editing:** Kevin A. Ryan, Thomas Adler, Ann Chalmers, Julia Perdrial, James B. Shanley, Aron Stubbins

& Germer, 2015). Quantifying the influence of vegetation on terrestrial to aquatic solute transfers within forested ecosystems is of particular importance because tree canopies are the primary interceptor of continental rainfall globally (Angelini et al., 2011).

Upon interacting with tree surfaces, precipitation becomes enriched in particulates and solutes (Michalzik & Stadler, 2005; Ponette-González et al., 2020). Throughfall comprises one of the largest internal water fluxes within forested ecosystems and delivers significant quantities of biogeochemically active water and solutes to the forest floor (McDowell et al., 2020). Stemflow delivers concentrated solutes to small areas surrounding tree trunks that influence local water and nutrient availability (Van Stan & Gordon, 2018) and can contribute to subsurface preferential flow paths (Johnson & Lehmann, 2016). Although stemflow volumes are modest, stemflow solute fluxes are generally more enriched in comparison to throughfall solute fluxes.

Within throughfall, dissolved organic carbon (DOC) comprises one of the largest solute fluxes by mass (McDowell et al., 2020) and is comparable to other important terrestrial carbon fluxes such as soil leaching and stream export (Stubbins et al., 2020). Concentrations of nitrogen species are also frequently elevated in throughfall and stemflow, although they are generally less enriched than DOC (Kristensen et al., 2004; Michalzik et al., 2001). The water, DOC, and nitrogen inputs from throughfall and stemflow can increase soil nutrient content (Klotzbücher et al., 2014; Qualls et al., 1991) and rates of forest litter decomposition (Qualls, 2020). In addition, stemflow from different tree species has been putatively associated with distinct soil microbial communities (Rosier et al., 2016) and throughfall can influence vegetation species composition through allelopathy (McDowell et al., 2020). The high spatial and temporal variability of throughfall and stemflow generates hot spots and hot moments of biogeochemical processing contributing to ecosystem control points that exert disproportionate influence on ecosystem function (Bernhardt et al., 2017; Van Stan & Stubbins, 2018).

Although tree-derived DOC initiates the aquatic carbon cycle in forested ecosystems, the extent to which carbon and nitrogen fluxes in throughfall and stemflow contribute to fluvial aquatic systems such as headwater streams and rivers is not well quantified. The high potential for alteration and loss of DOC along ill-defined subsurface flow paths and the high spatial and temporal variability of both tree-derived DOC and stream DOC fluxes contribute to this uncertainty (Van Stan & Stubbins, 2018). Ecosystem scientists have long recognized an excess of throughfall DOC inputs compared to stream exports within carbon budgets of small forested watersheds (Comiskey, 1978; McDowell & Likens, 1988). Early studies suggested that a significant amount of DOC in throughfall is respired by soil microbes or adsorbed to mineral soils (Qualls et al., 1991; Qualls & Haines, 1992), but that direct stream channel interception of throughfall for some storms could balance stream export (McDowell & Likens, 1988; Meyer & Tate, 1983). Since the primary DOC sources to streams are generally believed to be DOC in groundwater, riparian soils, and hillslopes connected to streams during storm events (Jansen et al., 2014), studies that attempt to link DOC dynamics in headwater streams to these sources commonly neglect consideration of direct throughfall inputs (Boyer et al., 1997; Hornberger et al., 1994; Zimmer & McGlynn, 2018). Throughfall DOC inputs have also been explicitly excluded in models of carbon transport and processing in streams (Dusek et al., 2017; Webster & Meyer, 1997) or combined with other compartments such as surficial soil layers when developing watershed carbon budgets (Argerich et al., 2016; Perdrial et al., 2018). More recent studies that have incorporated fluxes of tree-derived DOC into estimations of lateral carbon transport to aquatic systems are generally limited to monthly, seasonal, or annual comparisons (Johnson et al., 2006; Neu et al., 2016; Saunders et al., 2006; You et al., 2020).

Dissolved organic nitrogen, a component of dissolved organic matter present in throughfall, can comprise a significant portion (~50%) of total dissolved nitrogen (TDN) influencing nutrient balances in New England forested watersheds (Campbell et al., 2000). Both carbon and nitrogen sources in throughfall have also been included in end-member mixing analyses that have informed varied conclusions about the importance of throughfall chemistry on stream response (Brown et al., 1999; Hernes et al., 2017; Inamdar & Mitchell, 2006; Van Gaelen et al., 2014). For example, Sebestyen et al. (2019) used  $\delta^{18}\text{O-NO}_3$  measurements to confirm the rapid movement of unprocessed atmospheric nitrogen to streams during stormflow across a range of northern forested catchments, a finding most likely associated with throughfall flow pathways.

While annual or monthly carbon and nutrient export estimates for watersheds are useful, the need to assess carbon and nutrient fluxes at the event scale is increasingly apparent. For example, Raymond and Saiers (2010) estimated that 57% of annual DOC export from 30 small forested watersheds in the New England region (USA) occurred during larger hydrological events that accounted for just ~5% of the annual hydrograph. Carbon and other nutrient concentrations frequently increase with streamflow as water flushes large catchment stores (Moatar et al., 2017). Similarly, meteorological conditions of precipitation events influence the fluxes in throughfall and stemflow where solutes are generally diluted by increasing water input (Germer et al., 2007; Siegert et al., 2017), although not always. For example, Van Stan et al. (2017) observed that DOC concentrations in stemflow of epiphyte-laden oak trees in coastal Georgia containing proto-soils increased with precipitation magnitude, responding more like a miniature catchment. Thus, accurate annual estimates of DOC and nutrient fluxes in streams, throughfall and stemflow require the fluxes for individual hydrologic events to be determined and summed throughout the year. Event scale knowledge is therefore critical to predicting the impacts of changing event characteristics due to climate change on forested ecosystem function and surface water quality (Murdoch et al., 2000; Trenberth, 2011).

The apparent opposing influence of increasing precipitation event volume on throughfall and stream solute yields raises questions about how these event-based trends determine the net balance between tree-derived carbon and nitrogen inputs and stream exports for different seasons and hydrological conditions. Given the size of tree-derived DOC fluxes estimated to date, any fraction of throughfall and stemflow delivered directly to the stream during individual events could make important contributions to stream DOC export. Thus, improved estimates of tree-derived carbon and nitrogen fluxes are not only necessary to understand the factors modulating forest soil biogeochemistry but may also be relevant to in-stream and even distant downstream ecosystems (Van Stan & Stubbins, 2018).

In this study, we measured DOC and TDN concentrations in throughfall, stemflow and stream water for 23 events in a small, forested watershed. Using relationships established from the measured data, we modeled DOC and TDN event yields for each hydrologic flux for 76 events across a 2-year period. Our objectives were to: (a) assess inter-event variability of DOC and TDN event yields in throughfall, stemflow and stream water; (b) determine the influence of storm event size on throughfall, stemflow and stream DOC and TDN fluxes, and (c) compare tree-derived and stream fluxes at the event and annual scale. Our hypotheses were: (a) DOC and TDN concentrations in throughfall and stemflow will decrease with increasing rain event size; and (b) tree-derived DOC and TDN fluxes will exceed stream fluxes at both event and annual scales. To our knowledge, this is the first study to directly compare individual throughfall and stemflow event yields with corresponding stream event yields across annual time scales.

## 2. Materials and Methods

### 2.1. Study Site

The study site was Watershed 9 (W-9; Figure 1), a 41-ha headwater catchment within the Sleepers River Research Watershed in northeastern Vermont, USA. Sleepers River drains the rolling Kittredge Hills (total elevation range: 201–820 m) through forests and farmland to the Passumpsic River, a tributary of the Connecticut River. The mean annual temperature for the Sleepers River watershed is 6°C (W-9: 4.6°C), and snowfall comprises 20%–30% of annual precipitation (Shanley, 2000). The Sleepers River watershed, including W-9, is underlain by calcareous schist bedrock of the Waits River Formation and locally derived dense glacial till deposited ~10,000 years ago by the Wisconsinan glaciation (Springston & Haselton, 1999). W-9 is comprised of three main tributaries draining 155 m of elevation relief whose confluence forms the W-9 stream upstream of a concrete weir (Figure 1). The watershed is 100% forested, however, riparian wetlands and rock outcrops are present (Shanley et al., 2004). Trees in the watershed have not been selectively harvested since 1960 when it came under management of US governmental research agencies (Shanley et al., 2015). Dominant tree species are sugar maple (*Acer saccharum* Marsh.), yellow birch (*Betula alleghaniensis* Britt.), and white ash (*Fraxinus americana* Ehrh.), with minor amounts of balsam fir (*Abies balsamea* L.), red spruce (*Picea rubens* Sarg.), and American beech (*Fagus grandifolia* Ehrh.). A survey completed in 2011 of 404 living trees measured in 76 plots (100 m<sup>2</sup> each) across the watershed found that sugar maple and yellow birch comprised 75% and 11% of the total basal area, respectively (white ash = 8%). Mean diameter at breast height (DBH) for sugar maple and yellow birch was 26.4 cm ( $n = 296$ ) and 29.2 cm ( $n = 37$ ), respectively

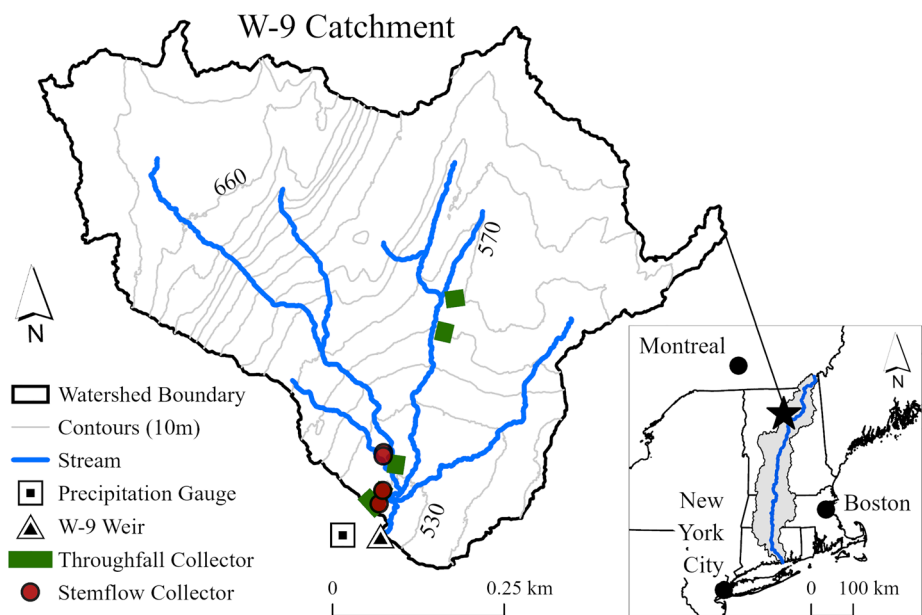


**Figure 1.** Sampling locations for precipitation, throughfall, stemflow and stream water in the W-9 watershed. Inset: The location of W-9 within the Connecticut River basin (gray shading) in the New England region of the USA (W-9 weir:  $44^{\circ}29'26''$  N,  $72^{\circ}09'44''$  W NAD27).

(white ash = 35.7 cm;  $n = 19$ ). The forest has not experienced significant tree stress or mortality from legacy acid deposition in the region due to the catchment's well-buffered soils (Shanley et al., 2004). Soils within W-9 are characterized as inceptisols, spodosols, and histosols, generally containing organic-rich surface horizons above loamy mineral horizons and a dense basal till (DeKett & Long, 1995).

## 2.2. Sample Collection and Processing

All sampling materials were precleaned with acidified deionized water (pH 2), triple rinsed with deionized water, and rinsed with sample water prior to collection. Grab samples were filtered immediately on site with 0.22  $\mu\text{m}$  filters (Polyethersulphone, Waterra). Stream water was sampled at the W-9 weir approximately weekly between May 2017 and December 2018. An ISCO automatic sampler triggered by stream stage was used to collect water from the W-9 weir pool during stream events. Samples collected by the automatic sampler were filtered on site upon collection within 24 h of an event. During the study period, 208 stream samples across a range of discharge conditions were collected (Figure 2).

Throughfall and stemflow were collected in W-9 for 23 rain events from June to November 2018 (Figure 2). Throughfall was collected along four transects of 3.0 m each and one transect of 12.2 m using aluminum troughs secured 80 cm above the forest floor and draining to plastic collection bins. Coarse plastic mesh covered the troughs to exclude leaves and other debris. Stemflow was collected from sugar maple (*Acer saccharum* Marsh.) and yellow birch (*Betula alleghaniensis* Britt) trees which together comprise the dominant hardwood species in the watershed (Park et al., 2008). Stemflow was collected from two mature trees of each species using low density polyethylene plastic collars sealed to the bark with silicone caulk. The stemflow tubing drained to a sealed plastic bucket. The depth of standing water in throughfall and stemflow collectors was measured after each rain event and converted to volume using a depth to volume calibration curve established for each collector type. Stemflow tree diameter at breast height ranged from 30 to 33 cm and canopy area ranged from 52 to 107  $\text{m}^2$  (Table S1). Throughfall and stemflow collectors were cleaned with a brush and deionized water prior to and after all measured precipitation events.

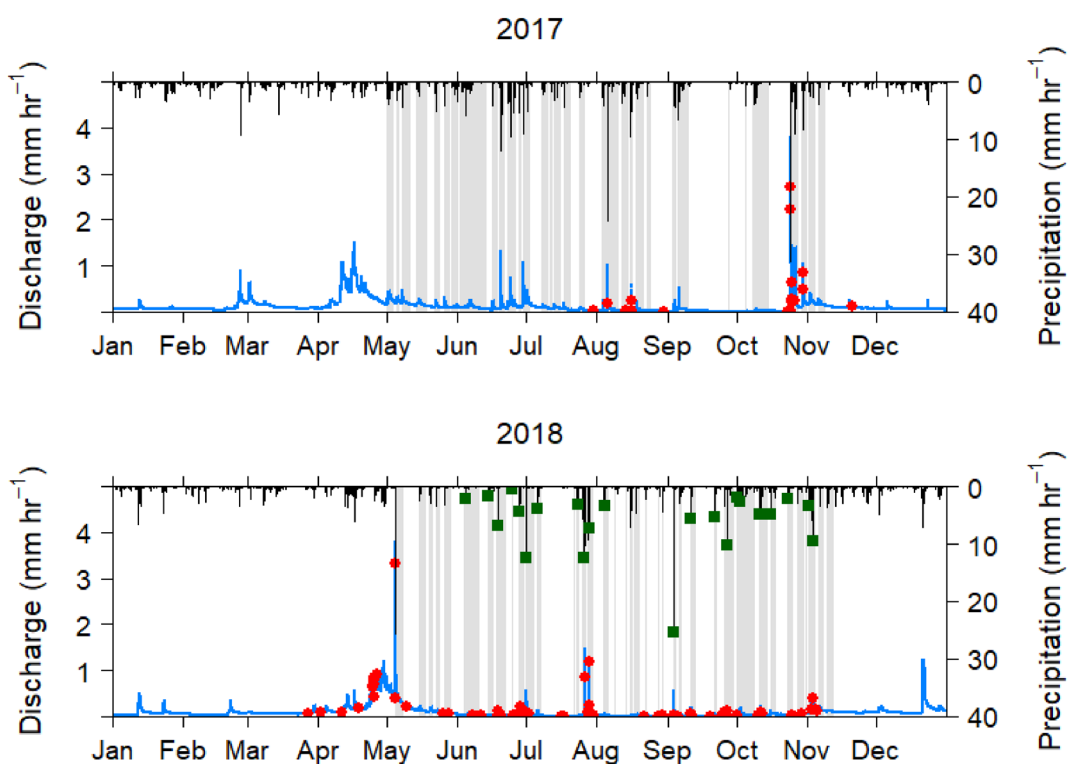


**Figure 2.** Time series of streamflow (blue) and precipitation (black) for Watershed #9 (W9) in the Sleepers River Research Watershed for 2017 and 2018 showing stream sampling times (red points) and the maximum precipitation intensity for sampled precipitation events (green squares). Delineated discharge and precipitation event pairs are shaded in gray. No events are shown for winter (November 15 to May 1) as snowfall was not sampled.

### 2.3. Dissolved Organic Carbon and Total Dissolved Nitrogen Concentrations

Aliquots of each sample for analysis of DOC and TDN were transferred to pre-combusted glass vials and acidified to pH 2 with 6N HCl and refrigerated (6°C) in the dark until analysis within 4 weeks of sampling. DOC was measured as non-purgeable organic carbon using a high-temperature catalytic combustion instrument (detection limit: 0.024 mg-C L<sup>-1</sup>; TOC-L by Shimadzu). TDN representing the sum of fixed forms of dissolved nitrogen (i.e., nitrate, nitrite, ammonium, and dissolved organic nitrogen), was measured by the TOC analyzer's TMN-L attachment (detection limit: 0.094 mg-N L<sup>-1</sup>). Calibration standards were prepared using a potassium hydrogen phthalate and potassium nitrate stock solution (1,000 mg-C L<sup>-1</sup>). Additionally, TDN concentrations were measured colorimetrically after in-line automated oxidation to nitrate at the Forestry Sciences Laboratory of the Northern Research Station (US Forest Service), according to the Lachat QuikChem E10-107-04-3-D method on a Lachat QuickChem 8500 (method detection limit: 0.05 mg-N L<sup>-1</sup>). TDN concentrations from the latter method were used when available and supplemented by Shimadzu measurements when unavailable.

### 2.4. Hydrometric Data Collection and Event Detection

The analysis was limited to rain and stream events identified between May 1 and November 15 of each year in order to exclude precipitation that fell as snow. Hourly precipitation for the watershed was recorded by two Belfort weighing-bucket rain gauges, one each at the lower elevation (528 m) and upper elevation (632 m) range of the watershed. Each electronic rain gauge record was processed according to Nayak et al. (2008) and amounts were prorated if necessary to match weekly observations from a National Weather Service non-recording standard rain gauge (203-mm diameter) at each site. The two records were combined via weighted basin hypsometry to generate a single precipitation record for the watershed (Shanley et al., 2004).

The W-9 stream gage is maintained by the US Geological Survey (USGS: site 01135100) and has a broad-crested concrete weir structure fitted with a 120-degree steel V-notch. Stream stage was measured by a potentiometer driven by a float and counterweight in a stilling well next to the weir pool and recorded at 5-min intervals by a datalogger. Stage was converted to discharge using an empirical rating curve derived from discharge measurements.

Precipitation event yields for measured events were calculated based on the start and end time of collection. The start and end time of the corresponding discharge events were manually selected within the period of throughfall and stemflow collection (Figure S1). Precipitation and stream flow events for the entire 2-year study period were delineated and paired algorithmically according to a 4-step procedure based on graphical hydrograph separation detailed in Text S1 (Figure S2; Multimedia S1).

### 3. Data Analysis

Event water yields of throughfall and stemflow were calculated by normalizing the volume of water collected to the surface area of the trough or the canopy area, respectively. Throughfall and stemflow event DOC and TDN yields were calculated by multiplying the event water yield by the concentrations in the bulk event water sample (Van Stan et al., 2017). To assess stemflow water yield efficiency and solute enrichment to the basal area for each tree with respect to precipitation and throughfall, dimensionless funneling ratios (FR) and flux-based enrichment ratios (ER) were calculated for each tree and stemflow event (Levia & Germer, 2015) (Equations 1–3),

$$FR = \frac{S_Y}{P \times B} \quad (1)$$

$$ER_{S,P} = \frac{S_Y \times C_S}{P \times B \times C_P} \quad (2)$$

$$ER_{S,T} = \frac{S_Y \times C_S}{T \times B \times C_T} \quad (3)$$

where  $S_Y$  is the stemflow event water yield ( $\text{mm}^3$ ),  $P$  is the precipitation event depth ( $\text{mm}$ ),  $B$  is the tree basal area ( $\text{mm}^2$ ),  $T$  is the throughfall event yield ( $\text{mm}$ ), and  $C_S$ ,  $C_P$ , and  $C_T$  are the concentrations of DOC and TDN in stemflow, precipitation, and throughfall, respectively. The flux-based enrichment ratios for DOC and TDN in throughfall compared to precipitation were also calculated (Equation 4).

$$ER_{T,P} = \frac{T \times C_T}{P \times C_P} \quad (4)$$

The influence of throughfall and stemflow collector locations and tree species on event water yields and concentrations were assessed using analysis of variance (ANOVA) and analysis of covariance (ANCOVA). All statistical analyses were completed in R using the “rstatix” package (version 0.6.0) (Kassambara, 2020). Robust methods for linear and nonlinear least squares estimation were implemented in R using the “robustbase” package (version 0.93–6) to fit linear and exponential decay models (Todorov & Filzmoser, 2009). Robust regression methods using iterated reweighted least squares were used to minimize the influence of rare large storms on the models. Nonlinear model error was estimated using first- and second-order Taylor expansion implemented in the “propagate” R package (version 1.0-6) (Spiess, 2018).

Continuous DOC and TDN stream loads were estimated using USGS LOADEST equations implemented within the “loadflex” R package (Appling et al., 2015; Aulenbach et al., 2016; Runkel & De Cicco, 2017; Runkel et al., 2004). Further details are provided in Text S2, Table S2, and Figures S4, S5, and S6. Stream event yields were calculated by summing the modeled 5-min DOC and TDN loads for the event period prior to normalizing to the watershed area.

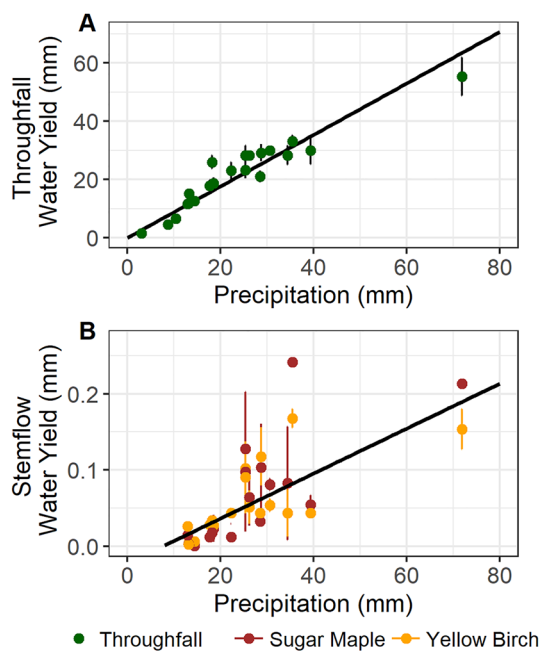


**Figure 3.** Water yields for (a) throughfall and (b) stemflow versus event precipitation. Error bars show 1 standard deviation from the mean of collector replicates. Throughfall robust linear model using event means with the intercept forced through zero:  $r^2 = 0.97$ ; slope =  $0.88 \pm 0.03$ ;  $p < 0.001$ . Stemflow robust linear model for both species combined using the mean event yields for each species:  $r^2 = 0.61$ ; slope =  $0.0030 \pm 0.0004$ ;  $y$ -intercept =  $-0.023 \pm 0.012$ ;  $x$ -intercept =  $7.6$ ;  $p < 0.001$ .

mean = 2.3; max = 6.4) generally increased with precipitation event size (Figure S3). The mean funneling ratio for yellow birch was significantly greater than the mean funneling ratio of sugar maple (ANOVA,  $F = 9.1$ ,  $p < 0.05$ ; Figure S3).

For subsequent modeling steps, the slopes of the linear correlations of throughfall and stemflow yield with precipitation event size were assumed to represent the overall proportion of precipitation converted to throughfall (88%) and stemflow (0.3%). All precipitation not converted to throughfall or stemflow was assumed lost to evaporation (Sadeghi et al., 2020).

The continuous stream discharge record spanned 2 years allowing delineation of stream discharge events during spring, summer, and autumn (Figure 2). The identified precipitation and discharge events pairs ( $n = 76$ ) ranged from 1.2 to 79 mm precipitation and 0.01–42 mm total event discharge. Combined precipitation-discharge event durations ranged from 6 to 270 h (mean =  $60 \pm 47$  h). The mean lag time between the start of precipitation and the start of the stream response was 3.5 h. Seven of the nine precipitation events that did not overlap with a detected stream event were small and occurred during the summer months of July, August, or September (precipitation event size range: 1.2–9.4 mm).

## 4. Results

### 4.1. Precipitation Partitioning and Hydrological Fluxes

Throughfall and stemflow were measured for 23 storm events ranging from 3 to 70 mm (median: 24 mm). Maximum hourly precipitation intensity within the measured rain events ranged from 0.5 to 25.0  $\text{mm hr}^{-1}$ . Measured event durations ranged from 3 to 43 h. Throughfall event water yield ranged from 1 to 62 mm (median: 22 mm). The means of the 5 throughfall collection sites of varying elevation were not significantly different from each other (ANOVA,  $F = 0.63$ ,  $p = 0.64$ ). The regression slopes of throughfall yield versus precipitation per event were also not significantly different among collection sites (ANOVA,  $F = 1.48$ ,  $p = 0.21$ ). Thus, data from the five throughfall collection sites were treated as replicates and averaged prior to further data analysis. Precipitation event size was a good predictor of throughfall event water yield (Linear regression:  $r^2 = 0.89$ ; slope =  $0.78 \pm 0.06$ ; intercept =  $3.02 \pm 1.77$ ;  $p < 0.001$ ). However, throughfall event water yield was forced through zero to avoid predicting greater throughfall than precipitation for small events (Figure 3a).

The minimum observed precipitation event size required to generate stemflow was 13 mm for both sugar maple and yellow birch trees, however the calculated  $x$ -intercept of the linear model was 7.6 mm (Figure 3b). Replicate stemflow water yields were averaged for each tree species and both species were included in a single linear model to predict increasing stemflow with increasing precipitation event size (Figure 3b). The maximum observed stemflow fraction of precipitation was 0.73%. Mean stemflow funneling ratios were greater than one indicating stemflow input to the forest floor at the tree's base generally exceeded mean areal rainfall amounts expected in the absence of the tree. Stemflow funneling ratios for sugar maple (median = 1.0; max = 5.2) and yellow birch (median = 1.0; max = 6.4) generally increased with precipitation event size (Figure S3). The mean funneling ratio for yellow birch was significantly greater than the mean funneling ratio of sugar maple (ANOVA,  $F = 9.1$ ,  $p < 0.05$ ; Figure S3).

### 4.2. Dissolved Organic Carbon and Total Dissolved Nitrogen Concentrations

DOC and TDN concentrations in stream water, throughfall, and stemflow were higher than in precipitation (Figure 4; ANOVA,  $p < 0.1$ ), although TDN concentrations in throughfall (mean  $\pm$  standard deviation (sd) =  $0.36 \pm 0.29 \text{ mg-N L}^{-1}$ ) were only moderately enriched compared to precipitation ( $0.20 \pm 0.16 \text{ mg-N L}^{-1}$ ). Both DOC and TDN concentrations in stemflow were significantly higher than in throughfall (Figures 4a and 4b; ANOVA,  $p < 0.001$ ). DOC concentrations in stemflow ranged widely from 7 to 195  $\text{mg-C L}^{-1}$  with sugar maple (mean  $\pm$  sd =  $57 \pm 44 \text{ mg-C L}^{-1}$ ) being more concentrated than yellow birch ( $38 \pm 25$ ).

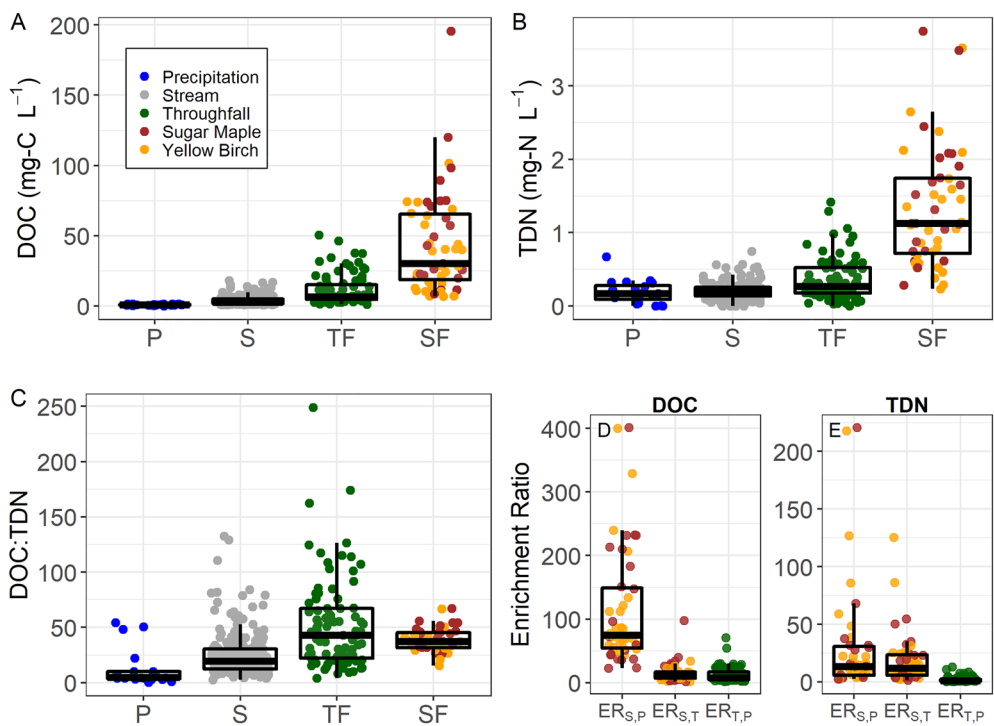


**Figure 4.** Boxplots and jitter plots of (a) dissolved organic carbon (DOC), (b) total dissolved nitrogen (TDN) and (c) molar DOC:TDN ratios for precipitation (P), stream water (S), throughfall (TF) and stemflow (SF) samples. All data from replicates are shown. Boxplots and jitter plots of flux-based enrichment ratios for stemflow with respect to precipitation ( $ER_{S,P}$ ), stemflow with respect to throughfall ( $ER_{S,T}$ ), and throughfall with respect to precipitation ( $ER_{T,P}$ ) for (d) DOC and (e) TDN. Boxes depict the median and first and third quartiles. Whiskers extend to the minimum or maximum value no further than 1.5 times the inner quartile range.

However, TDN concentrations in sugar maple ( $1.50 \pm 0.89 \text{ mg-N L}^{-1}$ ) and yellow birch ( $1.21 \pm 0.79 \text{ mg-N L}^{-1}$ ) were more similar.

Observations of DOC and TDN concentrations for the same storm event across replicate sites for throughfall and stemflow were averaged prior to further analysis as concentrations did not differ significantly among collection sites (ANOVA,  $p > 0.2$ ). Mean sugar maple stemflow DOC concentration was greater than mean yellow birch stemflow DOC concentration (ANOVA,  $F = 3.45$ ,  $p = 0.069$ ). There was no significant difference in mean TDN concentrations between the two tree species (ANOVA,  $F = 1.56$ ,  $p > 0.2$ ). To estimate stemflow event yields at the watershed scale, stemflow DOC and TDN concentrations were averaged across species for each event prior to further data analysis.

All waters were generally enriched in DOC relative to TDN. Mean ( $\pm$ standard deviation) molar DOC:TDN ratios for stream water ( $14 \pm 14$ ), throughfall ( $54 \pm 65$ ), sugar maple stemflow ( $39 \pm 13$ ), and yellow birch stemflow ( $34 \pm 14$ ) were greater than the mean ratio in precipitation ( $6.6 \pm 4.8$ ).

#### 4.3. Flux-Based Enrichment Ratios

The median flux-based enrichment ratios for DOC and TDN in throughfall with respect to precipitation ( $ER_{T,P}$ ) were 7.4 and 1.3, respectively. Median values are reported here to reduce the influence of skewness on the results (Figures 4d and 4e). Enrichment ratios for stemflow with respect to precipitation were similar among species and were higher for DOC (median  $ER_{S,P} \sim 74$ ) than for TDN (median  $ER_{S,P} \sim 14$ ) (Figures 4d and 4e). Median flux-based stemflow enrichment ratios with respect to throughfall ( $ER_{S,T}$ ) were more similar between DOC and TDN ranging from 8.0 to 13. No enrichment ratios were lower than 1.5.

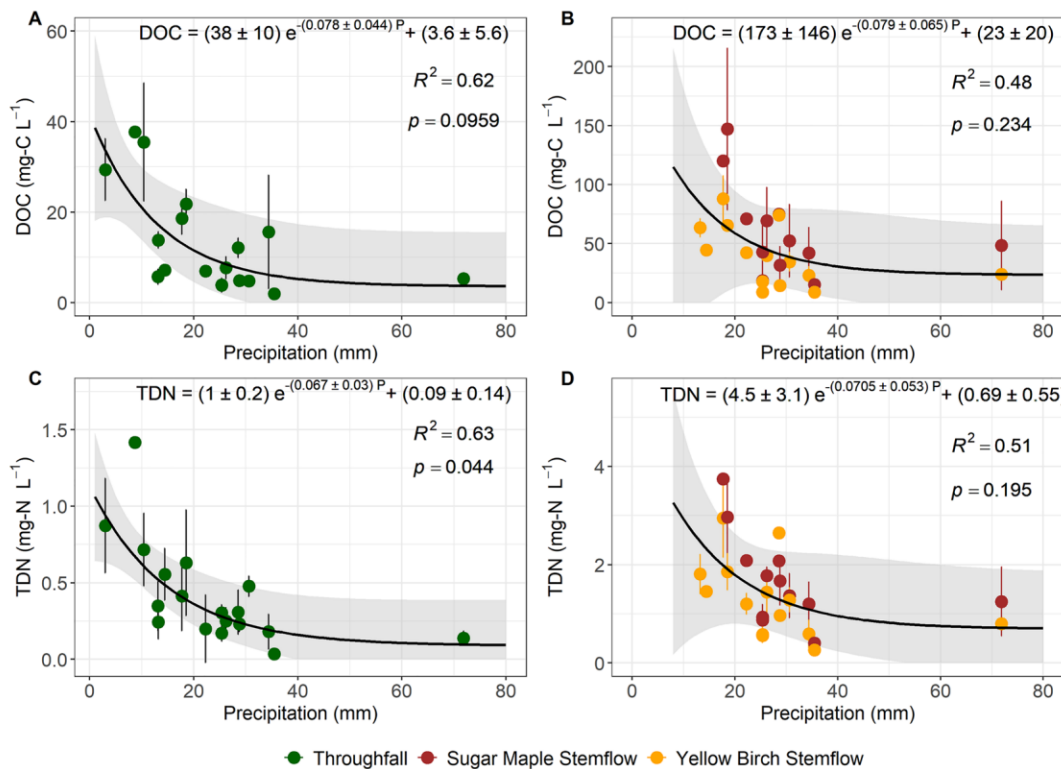


**Figure 5.** (a) Throughfall and (b) stemflow dissolved organic carbon (DOC), and (c) throughfall and (d) stemflow total dissolved nitrogen (TDN) versus event precipitation. Error bars show 1 standard deviation from the mean of replicate collectors per event. Exponential model coefficients and standard errors of each model coefficient are included on each plot. Gray shading corresponds to 95% confidence interval for the exponential decay model.

#### 4.4. Variability in DOC and TDN Concentrations With Event Size

Mean event DOC and TDN concentrations in throughfall and stemflow decreased with increasing storm size (Figure 5). Exponential decay models provided better statistical fits to the data than linear or log-linear models. Model error was estimated using first- and second-order Taylor expansion implemented in the “propagate” R package (version 1.0–6) (Spiess, 2018). Model equations and standard errors for each model term are reported in Figure 5. Models predict a reduction of 80%–90% of DOC and TDN concentration between a 1-mm event to an 80-mm precipitation event in both throughfall and stemflow. The sugar maple and yellow birch stemflow concentrations were modeled together due to strong similarities in yield and concentrations between the species (Figures 3b and 4). Stemflow was not modeled for precipitation events less than 7.6 mm, which was the  $x$ -intercept (i.e., the breakthrough volume) of the linear model for stemflow water yield (Figure 3b). The exponential term was similar for all models (range = 0.067 to 0.079  $\text{mm}^{-1}$ ) despite the wide range of DOC and TDN concentrations over event size between throughfall and stemflow.

#### 4.5. DOC and TDN Event Yields

DOC and TDN concentrations varied with discharge and season (Figure S4), thus discharge and decimal years were included as predictor variables within the LOADEST models ( $R^2 > 0.95$ ). Detailed model equations, coefficients, standard errors and calibration data and results are reported in Figures S5 and S6 and Table S2. Stream event DOC and TDN yields ( $\text{mg m}^{-2} \text{event}^{-1}$ ) were calculated by summing the modeled solute loads for each stream event period prior to dividing by the watershed area.

Modeled throughfall and stemflow DOC and TDN event yields for each of the 76 delineated events were calculated according to Equation 5:

$$\text{Event Yield} \left( \text{mg m}^{-2} \text{event}^{-1} \right) = aP \left( be^{cP} + d \right) \quad (5)$$

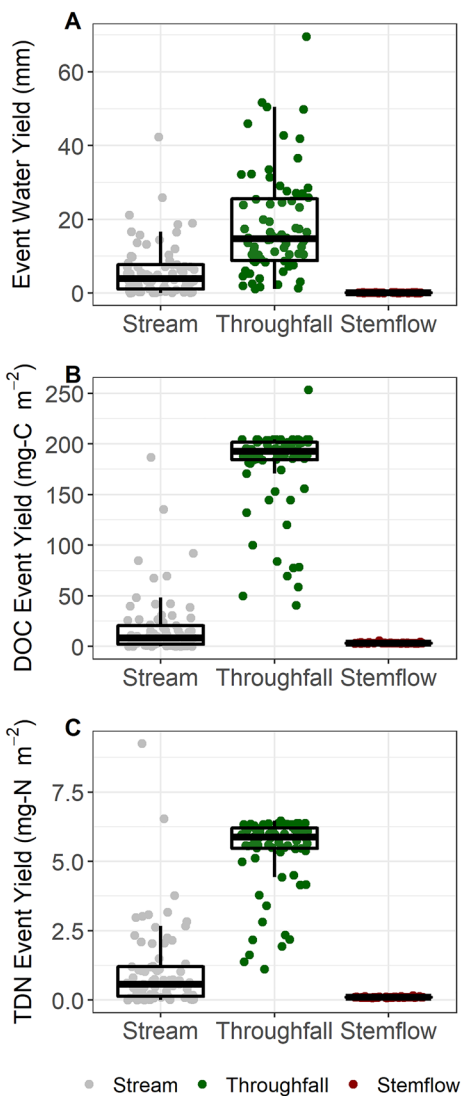


**Figure 6.** Box and jitter plots of modeled event yields in stream water, throughfall, and stemflow for (a) water, (b) dissolved organic carbon (DOC), and (c) total dissolved nitrogen (TDN). Boxes depict the median and first and third quartiles. Whiskers extend to the minimum or maximum value no further than 1.5 times the inner quartile range.

flow was detected (Figure 2; Multimedia S1). Stream event DOC yields approached throughfall yields only during the largest of events, suggesting a threshold of event size above which stream event export begins to approach throughfall inputs. A similar pattern was observed between throughfall and stream event TDN yields, although there was some evidence that large stream events export more TDN from the watershed than is delivered to soils via throughfall (Figure 7e).

Most stemflow event DOC and TDN yields were less than stream event yields (Figures 7d and 7f). However, some small rain events that were large enough to produce stemflow with high concentrations of DOC and TDN delivered these nutrients to basal soils in quantities greater than were exported from the watershed in the corresponding stream event (Figures 7d and 7f). Larger precipitation event sizes did increase stemflow event DOC and TDN yields, although the increases were marginal compared to increases in stream exports.

where  $a$  is the modeled fraction of event precipitation converted to throughfall or stemflow (0.88 and 0.03, respectively, Figure 3),  $P$  is event precipitation (mm), and  $b$  ( $\text{mg L}^{-1}$ ),  $c$  ( $\text{mm}^{-1}$ ) and  $d$  ( $\text{mg L}^{-1}$ ) are fitted coefficients for the exponential decay models predicting event concentrations (Figure 5). The uncertainty associated with individual event yields modeled using Equation 5 was estimated by propagating the standard errors of the model coefficients. Stemflow was assumed to be zero for precipitation events less than 7.6 mm (14 events; Figure 3b).

Modeled throughfall event water yields ( $\text{mean} \pm \text{sd} = 18 \pm 14 \text{ mm}$ ) were greater than the corresponding stream event water yields ( $\text{mean} \pm \text{sd} = 6 \pm 7 \text{ mm}$ ; Figure 6). The maximum modeled stemflow event water yield was 0.25 mm. Mean throughfall event DOC yield ( $172 \pm 42 \text{ mg-C m}^{-2}$ ) was nearly 10 times greater than mean stream event DOC yield ( $19 \pm 31 \text{ mg-C m}^{-2}$ ) and  $\sim 50$  times greater than mean stemflow event yield ( $3.5 \pm 0.4 \text{ mg-C m}^{-2}$ ). However, mean throughfall event TDN yields ( $5.3 \pm 1.3 \text{ mg-N m}^{-2}$ ) were more similar in magnitude to stream event TDN yields ( $1.1 \pm 1.5 \text{ mg-N m}^{-2}$ ). Maximum modeled stemflow event TDN yield was  $0.17 \text{ mg-N m}^{-2}$ .

#### 4.6. Comparison of Throughfall and Stemflow Event Yields With Stream Event Yields

To assess how the concentration and event yield relationships for throughfall and stemflow compare to the W-9 stream, tree-derived yields were plotted against their corresponding stream event yields (Figure 7). Values above the 1:1 line indicate greater input from throughfall or stemflow than stream export. For each event pairing, stream event water yields were nearly always at least 25% less than throughfall event water yields, but always 50% greater than stemflow event water yields (Figures 7a and 7b).

Similar to the comparison of water yields, throughfall event DOC yields were always greater than stream event DOC yields (Figure 7c). Throughfall and stream event DOC yields diverged the most for medium sized precipitation events ( $\sim 15$ – $30 \text{ mm}$ ) being more similar in magnitude for the smallest and largest precipitation events ( $\sim 10 > \text{event} > \sim 50 \text{ mm}$ ). For the smallest precipitation events, neither the canopy nor the stream exported large amounts of DOC. However, medium sized precipitation events can export significant amounts of DOC from the canopy even when flow paths controlling streamflow generation remain unconnected as evidenced by the nine precipitation events where no rise in stream-

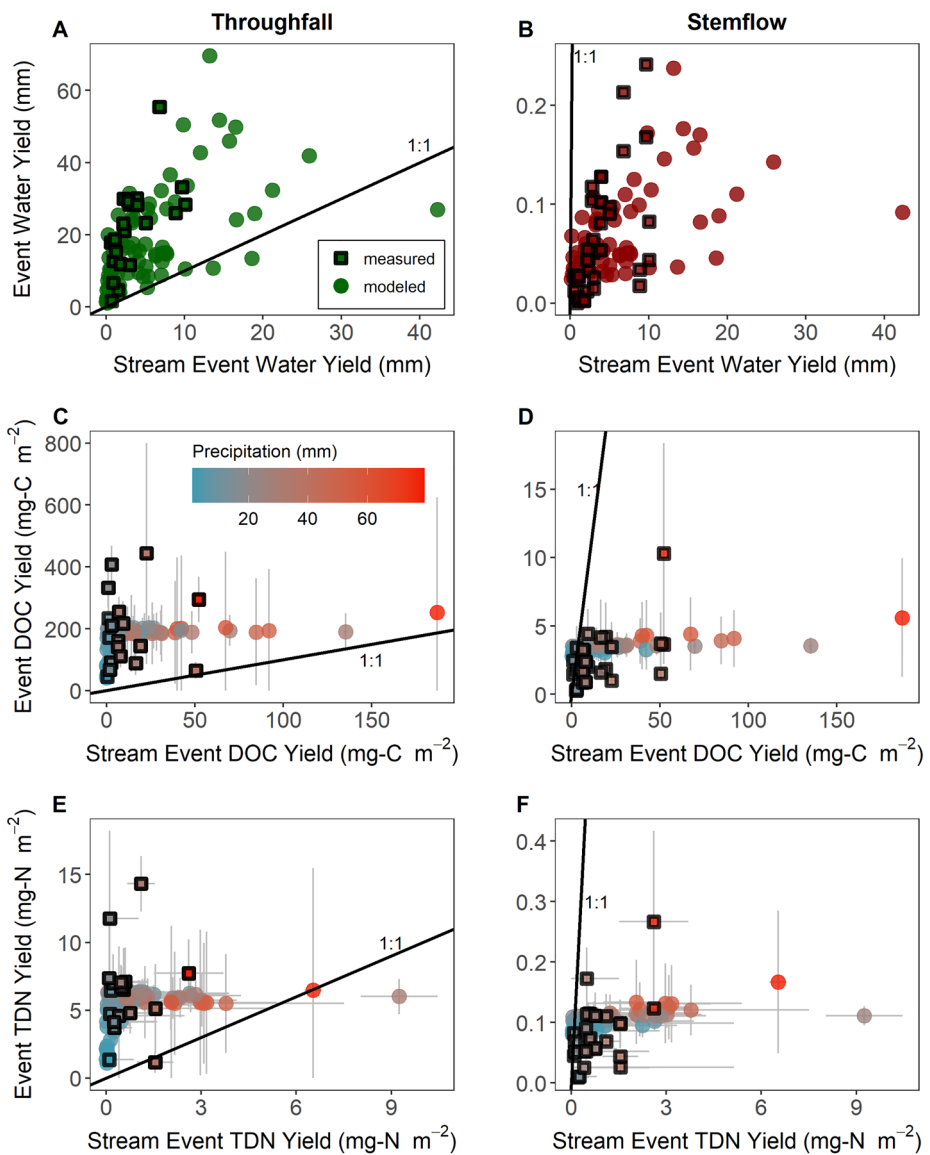


**Figure 7.** Event water yields versus paired stream event water yields for (a) throughfall and (b) stemflow. Event dissolved organic carbon (DOC) yields versus paired stream event DOC yields for (c) throughfall and (d) stemflow. Event total dissolved nitrogen (TDN) yields versus paired stream event TDN yields for (e) throughfall and (f) stemflow. Squares: mean of replicate collectors per measured event with vertical error bars representing 1 standard deviation of the replicate collectors. Circles: modeled events with vertical error bars representing propagated standard errors for model coefficients (Equation 5). All horizontal error bars are propagated root mean square errors for the LOADEST model summed for each event (Table S2). Data in C-F are colored by precipitation event size (scale in panel C). Stemflow yields for events <7 mm were estimated to be zero and are not shown. Values above the 1:1 line indicate greater input from throughfall or stemflow than stream export.

#### 4.7. Seasonal and Annual Yields

Annual stream yields were calculated by summing the precipitation, discharge, DOC and TDN continuous load records for the 2017 and 2018 calendar years and dividing by the watershed area (Table 1). Uncertainty for these sums is estimated by propagating the standard errors of each individual modeled event yield during summation for throughfall and stemflow events and by propagating the LOADEST model root mean square error for each stream event during summation. Mean precipitation concentrations were used to estimate annual precipitation yields. The discharge events identified during the study period (non-winter) exported ~20% to ~30% of annual discharge, but ~30% to ~50% of the annual DOC, and ~20% to ~40% of the

**Table 1**

*Total Yields of Water, Dissolved Organic Carbon (DOC), and Total Dissolved Nitrogen (TDN) for Precipitation, Stream, Throughfall and Stemflow Events During 2017 and 2018 Calendar Years*

		2017	2018
Water Yields mm	Precipitation	876 (1479)	692 (1371)
	Stream	289 (948)	164 (767)
	Throughfall	771	609
	Stemflow	3	2
DOC g·C m <sup>-2</sup> yr <sup>-1</sup>	Precipitation	0.83 ± 0.37	0.66 ± 0.29
	Stream	0.93 ± 0.027 (1.8 ± 0.1)	0.49 ± 0.025 (1.5 ± 0.1)
	Throughfall	6.6 ± 2.6	7.0 ± 1.7
	Stemflow	0.12 ± 0.036	0.12 ± 0.032
TDN g·N m <sup>-2</sup> yr <sup>-1</sup>	Precipitation	0.2 ± 0.13	0.15 ± 0.1
	Stream	0.053 ± 0.033 (0.13 ± 0.12)	0.028 ± 0.03 (0.12 ± 0.12)
	Throughfall	0.20 ± 0.058	0.21 ± 0.038
	Stemflow	0.0036 ± 0.0009	0.0036 ± 0.00079

*Note.* Uncertainty for modeled values is estimated via propagation of standard errors of model coefficients during summation. Estimates of throughfall and stemflow total yields do not include winter events occurring between November 15 and May 1. Annual yields that include winter and non-event periods are reported in parentheses when available.

Abbreviations: DOC, Dissolved organic carbon; TDN, Total dissolved nitrogen.

annual TDN yield. Annual yields of DOC and TDN exported from the canopy in throughfall and stemflow were only estimated for the non-winter study period (May 1 to November 15). The interactions of winter rain, snowfall, or ice with watershed vegetation were not assessed or estimated. For the non-winter period of study, total throughfall event DOC yields were ~7 to ~14 times greater than total stream event DOC yields during the same period while total stemflow event DOC yields comprised only a fraction of stream event DOC yields (~0.13 to ~0.24). Similarly, total throughfall event TDN yields were ~4 to 8 times greater than total stream event TDN export, with stemflow yields again being smaller (~0.07 to ~0.13).

Despite steady inputs of precipitation throughout the year, cumulative streamflow was marked by higher discharge during spring snowmelt and autumn recharge periods, with relatively lower water export during summer periods of peak evapotranspiration (Figure 8a). Cumulative throughfall and stemflow water yields (not shown in Figure 8a) were relatively constant throughout the study period since they were modeled as a linear function of precipitation. Annual accumulated stemflow DOC and TDN yields at the watershed scale were negligible in comparison to annual throughfall inputs or stream exports (Figures 8b and 8c). The accumulated DOC loading to the watershed in small and medium sized throughfall events greatly exceeded stream DOC export over the course of the study period (Figure 8b). The imbalance appears greatest during summer (July and August) when high evapotranspiration and low saturation of catchment soils limit stream export of water, DOC, and TDN. In contrast, these same summer storms deliver consistent fluxes of DOC and TDN from the canopy to the forest floor.

## 5. Discussion

### 5.1. Water Yields

Annual precipitation and streamflow (Table 1) were similar to long-term means for the watershed (precipitation: 1,330 mm, discharge: 760 mm) (Shanley et al., 2015). The two largest stream events occurred in fall (October 2017;  $P = 79$  mm, stream yield = 21 mm) and spring (May 2018;  $P = 37$  mm, stream yield = 42 mm). The 9 precipitation events that did not overlap with a detected stream response were small ( $P < 10$  mm) and seven of them occurred in the summer when high soil moisture deficits likely inhibited a stream response.

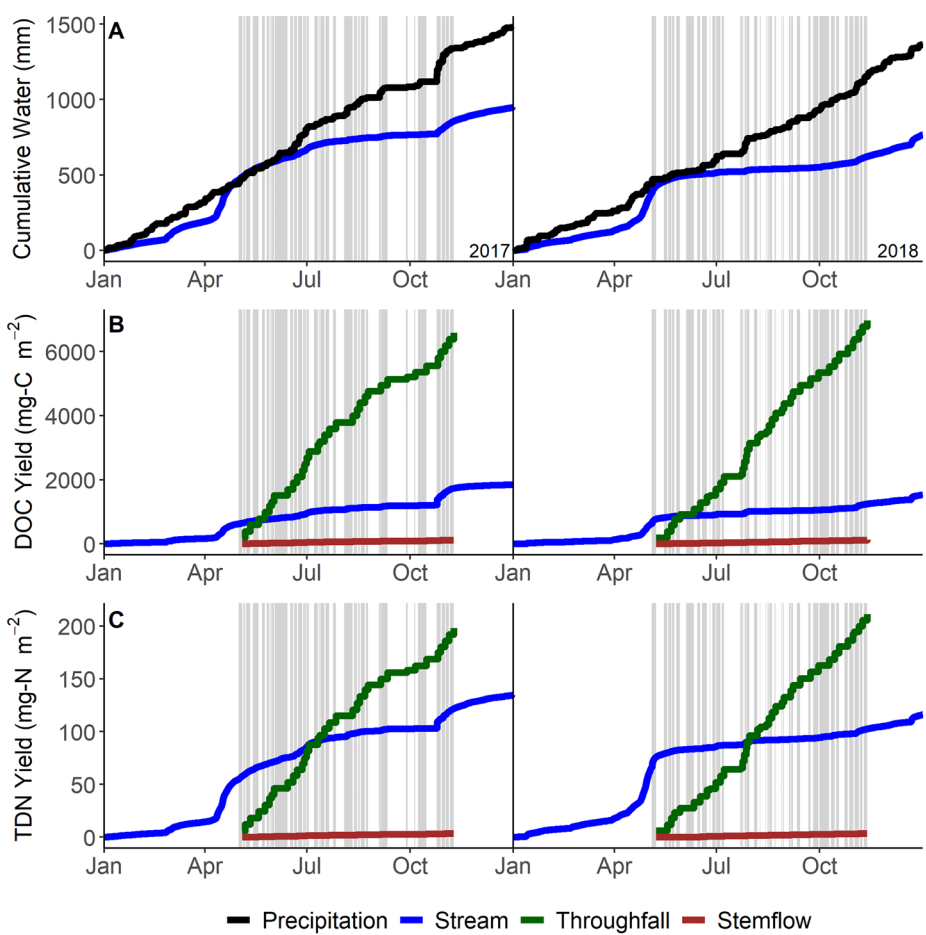


**Figure 8.** (a) Cumulative measured precipitation (black line) and streamflow (blue line) for the watershed during 2017 and 2018 calendar years. (b) Cumulative dissolved organic carbon (DOC) and (c) total dissolved nitrogen (TDN) yields in stream water (blue line), throughfall (green line) and stemflow (red line). Non-winter (May 1 to November 15) events are shaded in gray.

The modeled percentage of precipitation converted to throughfall (88%) was higher than that for forests globally (median 76%) (Sadeghi et al., 2020) but more similar to that for the nearby Hubbard Brook forest (~90%) (Leonard, 1961). Although event precipitation magnitude is commonly used to predict throughfall and stemflow water yield, additional influential factors include event intensity, wind direction, species and tree morphology (Levia & Frost, 2006; Levia & Germer, 2015).

The modeled stemflow yields (0.30%) fell within the lower range of those reported in previous studies globally (median 2.2%) (Sadeghi et al., 2020). Carlyle-Moses and Price (2006) observed sugar maple stemflow generation for rain events greater than 4.3 mm in Ontario, a lower threshold than the 7.6 mm value calculated in this study. The three observed precipitation events less than 13 mm occurred prior to complete installation of the stemflow collectors, thus additional observations could help to refine the minimum threshold of stemflow production within the study site. Stemflow funneling ratios (range: <1 to 6; Figure S3) fell near the lower range for deciduous trees (3–37) (Levia and Germer, 2015). Sugar maple funneling ratios (median = 1) were lower than those observed by Carlyle-Moses and Price (2006) (median = 22) in sugar maple trees of smaller basal areas (79–415 cm<sup>2</sup> vs. this study: 730–859 cm<sup>2</sup>). Yellow birch trees generated more stemflow per canopy area than sugar maple trees, likely due to differences in bark structure, where yellow birch bark is thin and smooth and sugar maple bark is thick and furrowed (Levia et al., 2010; Levia & Herwitz, 2005). For example, McGee et al. (2019) found that bark surface-moisture availability (g-H<sub>2</sub>O cm<sup>-2</sup> bark) increased with sugar maple bark thickness suggesting thicker bark adsorbs more water before stemflow generation begins. Additional factors influencing funneling ratio differences among individual

trees and species include differences in tree morphology such as branching angle, epiphyte cover, and storm damage (Levia & Germer, 2015; Sadeghi et al., 2020).

## 5.2. DOC and TDN Concentrations

Mean DOC concentration in precipitation (mean  $\pm$  sd =  $0.95 \pm 0.42$  mg-C L $^{-1}$ ) was within the range of means for continental rainfall globally ( $2.9 \pm 1.9$  mg-C L $^{-1}$ ) (Iavorivska et al., 2016), and similar to the long-term mean for precipitation at Sleepers River Research Watershed (1.14 mg-C L $^{-1}$ ). Mean TDN concentration in precipitation ( $0.22 \pm 0.15$  mg-N L $^{-1}$ ) was slightly lower than the long-term mean concentration (0.40 mg-N L $^{-1}$ ) for the watershed. Mean DOC and TDN concentrations in stream water (DOC =  $3.9 \pm 3.2$  mg-C L $^{-1}$ ; TDN =  $0.22 \pm 0.14$  mg-N L $^{-1}$ ) were similar to means reported previously in W-9 (DOC =  $4.1 \pm 3.1$  mg-C L $^{-1}$ ; TDN =  $0.23 \pm 0.21$  mg-N L $^{-1}$ ) (Sebestyen et al., 2014) and for temperate systems globally ( $\sim 4.0$  mg-C L $^{-1}$ ) (Mulholland, 2002). Molar DOC:TDN ratios in stream water ( $14 \pm 14$ ; Figure 4c) were also within the range reported in W-9 by Sebestyen et al. (2014) ( $\sim 2$ –100) and for rivers globally ( $33 \pm 16$ ) (Sipler & Bronk, 2015).

DOC concentrations in throughfall (mean  $\pm$  sd =  $12 \pm 11$  mg-C L $^{-1}$ ) and stemflow ( $54 \pm 65$ ) agreed with previous studies indicating that stemflow DOC (global range: 7 to 482) is generally more concentrated than throughfall DOC (1–61) (Van Stan & Stubbins, 2018). TDN concentrations in throughfall ( $0.36 \pm 0.29$  mg-N L $^{-1}$ ) and stemflow ( $1.2 \pm 0.9$ ) were similar to those reported for cedar and oak trees in Georgia USA ( $\sim 5$  mg-N L $^{-1}$ ) (Van Stan et al., 2017). Higher DOC concentrations in stemflow than throughfall may derive from increased contact time of water with tree surfaces and organic carbon sources combined with lower stemflow water yields (Stubbins et al., 2020). Although DOC and TDN concentrations were greater in stemflow than in throughfall, the DOC:TDN ratios were similar between the two flow paths (Figure 4c; median throughfall:  $\sim 34$ , median stemflow:  $\sim 35$ ), an observation in agreement with DOC:TDN values reported by Van Stan et al. (2017) ( $\sim 30$ –60) and suggests similar solute sources. Overall, DOC:TDN ratios indicated throughfall and stemflow were enriched in DOC relative to TDN and delivered carbon to the forest floor in excess of C:N ratios required for microbial growth ( $\sim 8.6$ ) (Cleveland & Liptzin, 2007).

## 5.3. Flux-Based Enrichment Ratios

Mean ( $\pm$ standard deviation) flux-based DOC enrichment ratios observed in this study for sugar maple and yellow birch stemflow relative to incident precipitation ( $ER_{S,P} = 110 \pm 88$  and  $122 \pm 102$ , respectively) were higher than those observed in a mixed cedar swamp in Ontario ( $ER_{S,P} = 16$  to 68) (Duval, 2019) and higher than those of an evergreen broad leafed stand in Japan (68) (Chen et al., 2019). Mean flux-based TDN enrichment ratios of stemflow relative to precipitation in this study (range =  $ER_{S,P} = 8.0$  to 16) were more similar to those reported by Duval (2019) (4.2–16). Stemflow  $ER_{S,P}$  for total nitrogen from a variety of research sites globally ranged from three in a tropical Costa Rican lowland rainforest to 44 in a South African Eucalyptus plantation (Levia and Germer, 2015). Mean stemflow enrichment ratios relative to throughfall ( $ER_{S,T}$ ) for DOC and TDN in this study (range = 17 to 20) were also higher than those reported by Duval (2019) (1–10). Stemflow  $ER_{S,T}$  for total nitrogen reviewed by Levia and Germer (2015) ranged from 3 to 39. Although not directly comparable to the TDN measurements in this study,  $ER_{S,P}$  for nitrate exceeded 2,000 for a tropical open rain forest in Brazil (Germer et al., 2012; Levia & Germer, 2015), but was less than 150 for a mixed oak-beech stand in Belgium (Andre et al., 2008). These results agree with previous studies indicating that stemflow input to forest soils at the base of trees exceed fluxes from incident rainfall and throughfall per unit trunk basal area.

## 5.4. Variability in DOC and TDN Concentrations With Event Size

DOC and TDN concentrations in stream water increased with increasing streamflow (Figure S4), a common pattern for streams that indicates watershed DOC and TDN export is generally limited by water availability for transport rather than supply of DOC and TDN (Moatar et al., 2017). Seasonal differences in DOC and TDN concentration response to streamflow incorporated into the stream load estimation model (Figures S4, S5 and S6; Table S2) agree with previous studies showing the flushing of carbon and nitrogen sources during spring snowmelt and autumn leaf fall periods (Sebestyen et al., 2008, 2014).

In contrast to streams, throughfall and stemflow DOC concentrations generally decreased with precipitation event size (Comiskey, 1978; Duval, 2019; Van Stan et al., 2017). This pattern has been described more widely for inorganic ions, although increases in concentrations of individual ions have been observed during events potentially driven by variable precipitation intensity and other factors (Hansen et al., 1994). Van Stan et al. (2017) reported continuously increasing DOC concentrations in the stemflow of epiphyte-laden live oak trees with increasing precipitation magnitude indicating DOC was transport limited rather than supply limited in those trees. In the current study, the exponential decrease in DOC and TDN concentration with increasing precipitation event magnitude is consistent with dilution by rain of sources available to be washed off or leached from tree surfaces during the event. Based upon dissolved organic matter quality, DOC in throughfall and stemflow likely derives from autochthonous (e.g., leaf, bark and epiphytic biota) and allochthonous sources (e.g., atmospheric deposition) deposited between storms (Stubbins et al., 2017). However, the influence of additional factors such as forest type and phenoseason on inter-storm variability in DOC export and quality is not well studied (Stubbins et al., 2020; Van Stan et al., 2017). Low variability of the exponential decay model slopes ( $c$  in Equation 5) fit to DOC and TDN concentrations for both throughfall and stemflow suggests a shared process (e.g., dilution by rainfall) drives the variability in DOC export (Figure 5). Exponential decay slopes modeled in this study ( $\sim 0.07 \text{ mm}^{-1}$ ) are higher than those reported by Duval (2019) ( $\sim 0.03 \text{ mm}^{-1}$ ) but lower than those reported in Van Stan et al. (2017) ( $\sim 0.1 \text{ mm}^{-1}$ ). However, slopes reported by Van Stan et al. (2017) may be influenced by the statistical treatment of binning data by rain event size prior to modeling. Future studies that capture more events, for more tree species across phenoseason and meteorological conditions are required to better define the factors controlling the export of DOC and TDN from tree surfaces.

### 5.5. DOC and TDN Yields

Annual stream DOC yields ( $1.5\text{--}1.8 \text{ g-C m}^{-2} \text{ yr}^{-1}$ ) were similar to those reported for 30 watersheds in New England, USA (mean = 2.4) (Raymond & Saiers, 2010). The two largest stream event DOC yields (0.19 and  $0.14 \text{ g-C m}^{-2} \text{ event}^{-1}$ ) were similar to the largest observed stream event in a forested watershed in Vermont ( $0.17 \text{ g-C m}^{-2} \text{ event}^{-1}$ ) (Vaughan et al., 2017), but less than the extreme events associated with hurricane Irene ( $0.3\text{--}0.6 \text{ g-C m}^{-2} \text{ event}^{-1}$ ) (Dhillon & Inamdar, 2013; Yoon & Raymond, 2012). Annual stream TDN yields ( $\sim 0.13 \text{ g-N m}^{-2} \text{ yr}^{-1}$ ) agreed with an estimate of annual stream export of dissolved inorganic nitrogen in W-9 (DIN =  $0.17 \text{ g-N m}^{-2} \text{ yr}^{-1}$ ) (Campbell et al., 2004). Both DOC and TDN stream yields increased with increasing rain event size as a result of increased water yields and increasing solute concentrations (Figure S7).

Annual throughfall DOC yields ( $\sim 7 \text{ g-C m}^{-2} \text{ yr}^{-1}$ ; Table 1) were similar to those reported in a deciduous oak forest in the Southern Appalachians USA ( $13 \text{ g-C m}^{-2} \text{ yr}^{-1}$ ) (Qualls et al., 1991), and in the Hubbard Brook watershed in New Hampshire USA ( $4 \text{ g-C m}^{-2} \text{ yr}^{-1}$ ) (McDowell & Likens, 1988). Throughfall and stemflow event DOC and TDN yields (Figure 7) were similar to those reported previously from cedar and oak trees in coastal Georgia ( $\sim 0.01\text{--}2 \text{ g-C m}^{-2} \text{ event}^{-1}$ ;  $0.1$  to  $150 \text{ mg-N m}^{-2} \text{ event}^{-1}$ ) (Van Stan et al., 2017) and a mixed cedar swamp in Ontario ( $\sim 0.1\text{--}0.5 \text{ g-C m}^{-2} \text{ event}^{-1}$ ;  $5$  to  $60 \text{ mg-N m}^{-2} \text{ event}^{-1}$ ) (Duval, 2019). Modeled throughfall DOC and TDN yields increased steadily for precipitation events  $<15 \text{ mm}$  as water yield increased by an order of magnitude (1–15 mm; Figure S7). However, in contrast to streams, throughfall yields for both DOC and TDN stabilized for precipitation events larger than  $\sim 15 \text{ mm}$ , although modeling errors for these events were greater. The pattern of a steady increase in DOC and TDN yield for small to medium sized storms followed by more stable yields for larger rain events is consistent with DOC yields observed by Duval (2019) and for cedar trees by Van Stan et al. (2017). This pattern indicates a fraction of DOC and TDN is removed from the canopy by new rainfall and is resupplied between events. Additional rainfall beyond  $\sim 15 \text{ mm}$  produced limited additional DOC and TDN yield corresponding to transportable reservoirs of about  $200 \text{ mg-C m}^{-2} \text{ event}^{-1}$  and  $\sim 5 \text{ mg-N m}^{-2} \text{ event}^{-1}$ . Although not assessed in this study, we expect transportable reservoirs of canopy nutrients to vary with event antecedent conditions, tree phenoseason, canopy biological activity, wind patterns and air quality.

### 5.6. Comparison of Throughfall and Stemflow Event Yields With Stream Event Yields

The ratio of event runoff to event precipitation (runoff coefficient: Q/P) allows watershed hydrological response to precipitation to be compared among events or watersheds (Blume et al., 2007). Event runoff coefficients for this study (range: 0.007 to 1.4) were consistent with previous observations in W-9 and indicate that event precipitation generally exceeds streamflow event response, although coefficients can vary by an order of magnitude depending on season and event size (Shanley et al., 2002). For example, the highest event runoff ratio was observed at the end of snowmelt, when stream discharge exceeded rainfall inputs (Q/P = 1.4; May 4, 2018), while the lowest value occurred when a small rainfall event fell upon the parched, summer catchment (Q/P = 0.007; July 22, 2018).

Runoff coefficients calculated as event streamflow divided by combined throughfall and stemflow (Figures 7a and 7b) represent the efficiency of transfer of water from the forest floor to the stream and are higher than Q/P calculated using incident precipitation. In some cases, the ratio approaches 100%, indicating that sometimes streams export as much water as falls upon the forest floor. Overall, the comparison of throughfall and stream event water yields indicate a disconnection between canopy flow paths and the stream, where soils and non-stream flow paths buffer the water response from canopy to streams. Thus, improved understanding of water transfer from canopy to forest floor appears critical to improved modeling of water and solute fluxes through forest ecosystems to their streams.

An increase in carbon export in streams with increasing precipitation event size due to more connectivity of water and watershed carbon sources has been well described in previous studies (Dhillon & Inamdar, 2013; Raymond & Sayers, 2010). The dilution of DOC and TDN concentrations in throughfall and stemflow with increasing precipitation input oppose the concentrating pattern in streams with increasing streamflow (Figures 5, 9a and 9b). Thus, these diverging relationships for concentrations drive differences in patterns of event yields between throughfall, stemflow and streams explaining the convergence of throughfall and stream DOC event yields for large storms.

### 5.7. Comparison of Cumulative and Annual Watershed Fluxes

The linear models used in this study to predict throughfall and stemflow water yield (Figure 3) may overestimate yields for small storms where a greater fraction of precipitation is lost to interception (Carlyle-Moses & Gash, 2011). Although non-linear models that do not use a fixed fraction of throughfall and stemflow can improve predictions (Zwanzig et al., 2020), they require more data than are available in the current study. In addition, modeled stemflow event water yields were generally higher than measured stemflow event water yields due to negative residuals present in the stemflow water yield model (Figure 3b). This overestimation minimally influenced the comparison with stream event yields because stemflow event water yields were a minor hydrologic flux compared to throughfall, and stemflow is not delivered to soils at all for the smallest rain events (Figure 8).

Modeled event pairings could not be directly compared to measured event pairs because measured events were chosen based on logistical constraints associated with discontinuous sampling, while modeled events were delineated within the continuous records for precipitation and streamflow (Text S1). Modeled DOC and TDN throughfall and stemflow yields were estimated based solely upon relationships with rain event size. Other factors that can modulate throughfall and stemflow nutrient fluxes, such as phenoseason (Sadeghi et al., 2020), were not considered due to limited data. The LOADEST model for streams was driven by variation in discharge and season. Thus, seasonal variation in our model results reflect seasonal differences in modeled stream fluxes, plus any seasonal distribution of event size and frequency across the study period. Despite these limitations, the comparison of watershed inputs and exports at the event scale reveals the influence of storm size on the hydro-biogeochemical processes controlling the relative fluxes of DOC and TDN in throughfall, stemflow and streams as discussed below.

The combined throughfall and stemflow DOC yields during the non-winter period ( $\sim 7 \text{ g-C m}^2 \text{ yr}^{-1}$ ) are larger than annual stream DOC yields ( $\sim 2 \text{ g-C m}^2 \text{ yr}^{-1}$ ; winter included), but minor in comparison to estimates of annual litterfall ( $\sim 150 \text{ g-C m}^2 \text{ yr}^{-1}$ ) and aboveground woody biomass production in W-9 ( $\sim 400 \text{ g-C m}^2 \text{ yr}^{-1}$ ) (Park et al., 2008). Throughfall DOC yield for the non-winter period is equivalent to less than 2% of net primary production estimates for New England forests ( $\sim 400 \text{ g-C m}^2 \text{ yr}^{-1}$ ) (Tang et al., 2010)

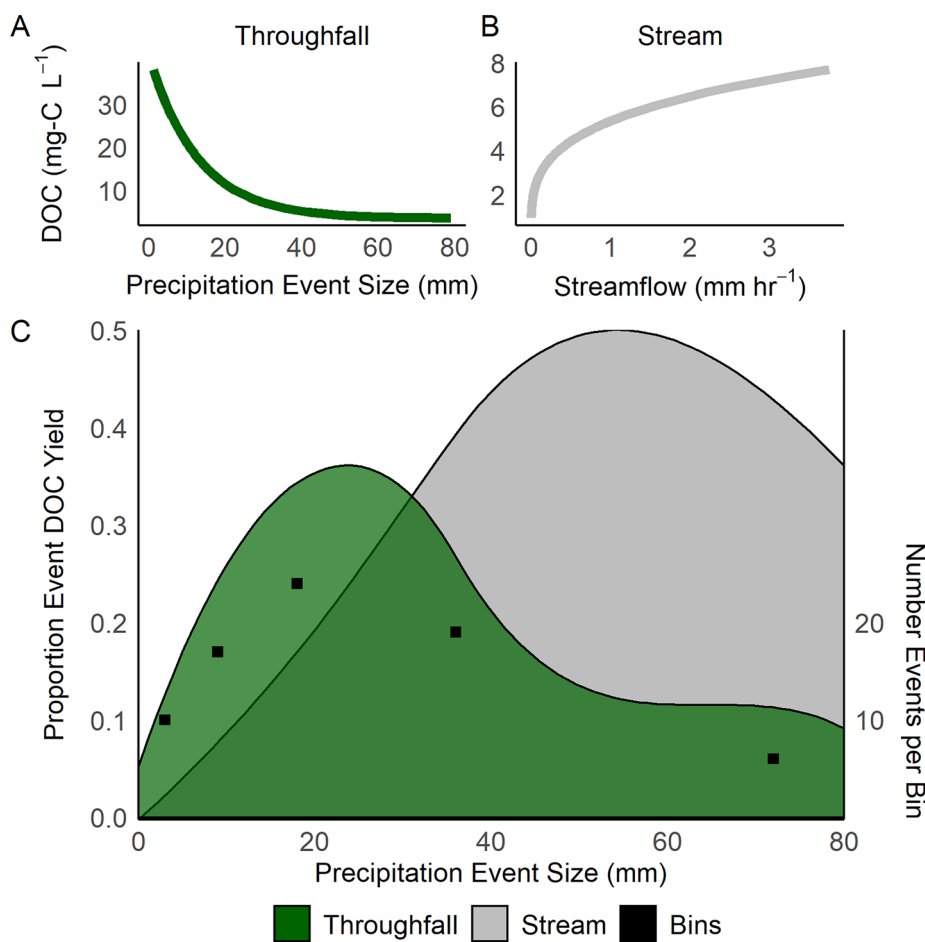


**Figure 9.** Example of opposing concentration dynamics between (a) throughfall and (b) stream water during events. (c) Estimated proportion of event DOC yield across precipitation event size that contributed to the total event yield during the non-winter study period. Proportions were calculated by grouping events into 5 bins based on precipitation event size prior to dividing the total yield for each group by the total event yield for the study period. Events greater than 48 mm were placed in the highest group, and the bounds on each lower bin were determined by dividing the proceeding bound in half (e.g., 48, 24, 12, 6, 3 ... 0). Results are displayed as locally weighted smoothed lines. Similar results for TDN and stemflow are shown in Figure S8.

and represents  $\sim 5\%$  of estimates of annual net ecosystem exchange for the nearby Hubbard Brook forest in New Hampshire ( $132 \pm 49 \text{ g-C m}^2 \text{ yr}^{-1}$ ) (Ouimette et al., 2018). However, throughfall and stemflow DOC yields are more similar to estimates of DOC leached from the organic horizon of forested soils in the New England region ( $22.5\text{--}26.3 \text{ g-C m}^2 \text{ yr}^{-1}$ ) (Michalzik et al., 2001). The molar DOC:TDN ratios in throughfall and stemflow ( $\sim 25\text{--}75$ ) are also more similar to soil leachates (DOC:DON =  $26 \pm 10$ ) (Michalzik et al., 2001) than to litter (C:N =  $\sim 50$  to 100) or woody debris (C:N =  $\sim 10^2$  to  $10^3$ ) (Manzoni et al., 2010). Although throughfall and stemflow create hotspots of biogeochemical processing, the delivery of DOC and TDN in throughfall and stemflow to the forest floor is more consistent throughout the non-winter period observed in this study compared to the larger autumnal inputs of litter fall and woody debris. The frequent delivery of water, labile organic carbon, and nitrogen from throughfall and stemflow has the potential to support background metabolic activity in soils. However, distinguishing the relative influence of new water inputs and chemical subsidies on forest floor biogeochemistry remains a challenge (Qualls, 2020).

Given the imbalance between throughfall inputs and stream exports, the majority of tree-derived DOC delivered to the forest floor is likely respiration in soils, lost to other flow paths (e.g., groundwater), or enters storage as net ecosystem production or accumulation. DOC in throughfall is highly biolabile ( $\sim 30\text{--}70\%$  over several days) (Howard et al., 2018; Qualls & Haines, 1992). However, how the biolability of DOC in

a laboratory incubation translates to rates of DOC loss in the soil is unclear. Decreasing concentrations of DOC in soil leachate down soil depth profiles indicate that ~50% of DOC is removed from solution within mineral soils (Cronan & Aiken, 1985; McDowell & Wood, 1984), an observation supporting conceptual models proposing that longer, deeper subsurface flow paths buffer stream response to throughfall DOC inputs (McDowell & Likens, 1988; Neff & Asner, 2001). Results from end-member mixing studies suggest at least some throughfall DOC reaches the stream, typically contributing to streamflow early in the event (Dhillon & Inamdar, 2013). Similarly, isotopic evidence indicates unaltered atmospheric nitrate appears in stormflow in W-9 and may be delivered by rapid routing of precipitation through terrestrial flow paths (Sebestyen et al., 2014). Thus, despite the well-established loss mechanisms, whether a fraction of throughfall and stemflow contribute substantially to stream event solute fluxes and how this delivery varies with event characteristics such as precipitation magnitude and intensity remains an open question.

Rapid transfer of canopy solutes to streams can occur via direct interception of throughfall by stream channels or saturated riparian areas (McDowell & Likens, 1988; Meyer & Tate, 1983). Given the magnitude of throughfall DOC yields compared to stream DOC yields, <10% of watershed area is needed to route throughfall DOC directly to the stream via surficial flow paths (e.g., direct channel interception, saturated overland flow, or shallow soil macropore flow) to generate the mass of DOC exported by the stream, particularly for smaller events and at the onset of all events. This represents an area comparable to the extent of combined channel and saturated riparian areas typical of small, forested watersheds (McGlynn et al., 2004). We found that the first 10 mm of throughfall contains the bulk of tree-derived DOC input to the forest floor (Figure S7), supporting the argument by Meyer and Tate (1983) and others that direct throughfall contributions to streams is most likely to occur on the rising limb of the storm hydrograph (Inamdar et al., 2013; Inamdar & Mitchell, 2007). However, DOC concentrations in the W-9 stream and other temperate streams typically remain elevated after peak discharge (Shanley et al., 2015), suggesting additional DOC sources such as surficial soils are contributing on the falling limb of the storm hydrograph. The current study demonstrates that the potential for throughfall and stemflow DOC and TDN to reach the stream varies with rain event size and potentially seasons. Determining the extent to which throughfall DOC input is decoupled from stream DOC export at the scale of individual storm events requires detailed assessment of watershed hydrological flow paths and their timing, an undertaking that continues to challenge the field of catchment hydrology (Tetzlaff et al., 2015).

### 5.8. Implications for Climate Change

Climate change is increasing temperature, growing season length, precipitation, and storm intensity in the New England region (USA) (Feng et al., 2016; Huntington et al., 2009; Parr and Wang, 2014) and climate related increases in stream carbon and nitrogen export have already been reported for W-9 (Sebestyen et al., 2009). Given the relatively high DOC yields in throughfall and stemflow for small events (<~20 mm), frequent small storms provide the bulk of DOC inputs from throughfall and stemflow to the forest floor (Figure 9c). The opposite is generally true for the W-9 stream and for New England rivers where infrequent, large storms can export a majority of annual DOC (Raymond et al., 2016). Thus, the distribution of hydrologic event frequency and intensity across seasons is likely an important factor influencing annual carbon budgets, especially for mid-to-high latitude regions (Laudon et al., 2013).

Winters in the northeastern USA are of particular importance for ecosystem processes as they experience greater relative warming due to climate change (Campbell et al., 2005; Kreyling, 2020). Further study of carbon and nitrogen fluxes from vegetation and streams during winter periods is warranted especially since stemflow solute fluxes are sensitive to winter meteorological event type (Levia, 2003). Wilcke et al. (2020) reported a climate-related decrease in total organic carbon concentration in throughfall from 1998 to 2013 in a tropical montane forest while concentrations in stemflow increased over the same period suggesting that climate change may influence throughfall and stemflow differently. Thus, improved understanding of how throughfall, stemflow and stream solute export varies with precipitation event characteristics is critical to assessing the sensitivity of these ecologically important biogeochemical fluxes to climate forcing.

## 6. Conclusion

We report the first throughfall and stemflow water, DOC and TDN yields in the Sleepers River Research Watershed. Modeled throughfall and stemflow event DOC and TDN yields were paired with modeled stream event yields for a 2-year period to compare event scale variation in throughfall, stemflow and stream event yields. Throughfall, stemflow and stream water were significantly enriched in DOC and TDN relative to precipitation. DOC and TDN concentrations increased with streamflow, while their concentrations in throughfall and stemflow decreased exponentially with increasing precipitation (Figures 5, 9a, and 9b). We interpret these relationships to indicate that solutes were washed and leached from tree surfaces ultimately being diluted by rainwater, whereas the streams were limited by water availability for transport of catchment stores of carbon and nitrogen.

Total annual throughfall DOC and TDN yields for the non-winter periods of study were  $\sim$ 2–5 times greater than total stream yields for the entire year, while annual stemflow yields comprised less than 10% of total annual stream yields (Table 1; Figure 8). Most individual medium sized rainfall events (15–30 mm) exported  $\sim$ 10 to 40 times more DOC to the forest floor than was exported by their paired stream events, while throughfall yields for larger events were  $\sim$ 2–6 times greater than streams yields (Figures 7c and 7e). For instance, the largest 10 stream events exported  $\sim$ 40% of all stream event DOC whereas those same 10 events contributed  $\sim$ 14% of all throughfall export. The strong but contrasting influence of rain event size on throughfall, stemflow and stream solute yields is likely an important driver of the relative balance of watershed inputs and exports annually. Thus, the distribution of event size and frequency across seasons has important implications for annual carbon and nitrogen budgets. Long term trends in event frequency and intensity may influence annual ecosystem function by concentrating hot moments of carbon mobilization from the canopy into soils during the summer when soil microbial activity is greatest and stream exports are minimal. In contrast, increased frequency of large storms is likely to favor watershed export (Figure 9c). Further, tree-derived solutes that do contribute to stream fluxes during storm events could be rapidly shunted to downstream aquatic ecosystems (Raymond et al., 2016; Van Stan and Stubbins, 2018). As land use and climate change continues to alter hydrologic event characteristics and forest structure (Duvaneck et al., 2016; Trenberth, 2011), improved mechanistic understanding of event controls on watershed fluxes is critical to understand future ecosystem and carbon cycle function of forests, their soils and the streams that drain them.

## Data Availability Statement

Data are publicly available in the USGS Science Base data repository (Ryan et al., 2021).

## Acknowledgments

The authors thank Miles Despathy, Russell Desclos, and Jon Denner for assistance with field measurements. The authors thank Bryan Yoon, John Van Stan, Amy Mueller, Jake Hosen and USGS internal reviewers for discussions that improved data analysis and writing. The authors thank Jenn Fair for her review of an earlier version of this study as well as two anonymous reviewers. Any use of trade, firm, or product names is for descriptive purposes only and does not imply endorsement by the U.S. Government.

## References

Andre, F., Jonard, M., & Ponette, Q. (2008). Effects of biological and meteorological factors on stemflow chemistry within a temperate mixed oak-beech stand. *Science of the Total Environment*, 393(1), 72–83. <https://doi.org/10.1016/j.scitotenv.2007.12.002>

Angelini, I. M., Garstang, M., Davis, R. E., Hayden, B., Fitzjarrald, D. R., Legates, D. R., et al. (2011). On the coupling between vegetation and the atmosphere. *Theoretical and Applied Climatology*, 105(1–2), 243–261. <https://doi.org/10.1007/s00704-010-0377-5>

Appling, A. P., Leon, M. C., & McDowell, W. H. (2015). Reducing bias and quantifying uncertainty in watershed flux estimates: The R package loadflex. *Ecosphere*, 6(12), 269. <https://doi.org/10.1890/es14-00517.1>

Argerich, A., Haggerty, R., Johnson, S. L., Wondzell, S. M., Dosch, N., Corson-Rikert, H., et al. (2016). Comprehensive multiyear carbon budget of a temperate headwater stream. *Journal of Geophysical Research: Biogeosciences*, 121(5), 1306–1315. <https://doi.org/10.1002/2015jg003050>

Aulenbach, B. T., Burns, D. A., Shanley, J. B., Yanai, R. D., Bae, K., Wild, A. D., et al. (2016). Approaches to stream solute load estimation for solutes with varying dynamics from five diverse small watersheds. *Ecosphere*, 7(6). <https://doi.org/10.1002/ecs2.1298>

Bernhardt, E. S., Blaszcak, J. R., Ficken, C. D., Fork, M. L., Kaiser, K. E., & Seybold, E. C. (2017). Control points in ecosystems: Moving beyond the hot spot hot moment concept. *Ecosystems*, 20(4), 665–682. <https://doi.org/10.1007/s10021-016-0103-y>

Blume, T., Zehe, E., & Bronstert, A. (2007). Rainfall—Runoff response, event-based runoff coefficients and hydrograph separation. *Hydrological Sciences Journal*, 52(5), 843–862. <https://doi.org/10.1623/hjs.52.5.843>

Boyer, E. W., Hornberger, G. M., Bencala, K. E., & McKnight, D. M. (1997). Response characteristics of DOC flushing in an alpine catchment. *Hydrological Processes*, 11(12), 1635–1647. [https://doi.org/10.1002/\(sici\)1099-1085\(19971015\)11:12<1635::aid-hyp494>3.0.co;2-h](https://doi.org/10.1002/(sici)1099-1085(19971015)11:12<1635::aid-hyp494>3.0.co;2-h)

Brown, V. A., McDonnell, J. J., Burns, D. A., & Kendall, C. (1999). The role of event water, a rapid shallow flow component, and catchment size in summer stormflow. *Journal of Hydrology*, 217(3–4), 171–190. [https://doi.org/10.1016/s0022-1694\(98\)00247-9](https://doi.org/10.1016/s0022-1694(98)00247-9)

Campbell, J. L., Hornbeck, J. W., McDowell, W. H., Buso, D. C., Shanley, J. B., & Likens, G. E. (2000). Dissolved organic nitrogen budgets for upland, forested ecosystems in New England. *Biogeochemistry*, 49(2), 123–142. <https://doi.org/10.1023/a:1006383731753>

Campbell, J. L., Hornbeck, J. W., Mitchell, M. J., Adams, M. B., Castro, M. S., Driscoll, C. T., et al. (2004). Input-Output budgets of inorganic nitrogen for 24 forest watersheds in the northeastern United States: A review. *Water, Air, and Soil Pollution*, 151(1–4), 373–396. <https://doi.org/10.1023/b:Water.000009908.94219.04>

Campbell, J. L., Mitchell, M. J., Groffman, P. M., Christenson, L. M., & Hardy, J. P. (2005). Winter in northeastern North America: A critical period for ecological processes. *Frontiers in Ecology and the Environment*, 3, 314–322. [https://doi.org/10.1890/1540-9295\(2005\)003\[0314:winnaa\]2.0.co;2](https://doi.org/10.1890/1540-9295(2005)00310.18.90/1540-9295(2005)003[0314:winnaa]2.0.co;2)

Carlyle-Moses, D. E., & Gash, J. H. C. (2011). Rainfall Interception Loss by Forest Canopies. In *Forest hydrology and biogeochemistry* (pp. 407–423). [https://doi.org/10.1007/978-94-007-1363-5\\_20](https://doi.org/10.1007/978-94-007-1363-5_20)

Carlyle-Moses, D. E., & Price, A. G. (2006). Growing-season stemflow production within a deciduous forest of southern Ontario. *Hydrological Processes*, 20(17), 3651–3663. <https://doi.org/10.1002/hyp.6380>

Chen, S., Cao, R., Yoshitake, S., & Ohtsuka, T. (2019). Stemflow hydrology and DOM flux in relation to tree size and rainfall event characteristics. *Agricultural and Forest Meteorology*, 279, 107753. <https://doi.org/10.1016/j.agrformet.2019.107753>

Cleveland, C. C., & Liptzin, D. (2007). C:N:P stoichiometry in soil: Is there a “Redfield ratio” for the microbial biomass? *Biogeochemistry*, 85(3), 235–252. <https://doi.org/10.1007/s10533-007-9132-0>

Comiskey, C. E. (1978). *Aspects of the organic carbon cycle on Walker branch watershed: A study in land/water interaction*. (Doctoral thesis) (p. 509). University of Tennessee.

Cronan, C. S., & Aiken, G. R. (1985). Chemistry and transport of soluble humic substances in forested watersheds of the Adirondack Park, New York. *Geochimica et Cosmochimica Acta*, 49(8), 1697–1705. [https://doi.org/10.1016/0016-7037\(85\)90140-1](https://doi.org/10.1016/0016-7037(85)90140-1)

DeKett, R. G., & Long, R. F. (1995). *Order 1 soil mapping Project of the W-9 basin in the Sleepers River watershed*. (p. 66). United States Department of Agriculture Natural Resources Conservation Service.

Dhillon, G. S., & Inamdar, S. P. (2013). Extreme storms and changes in particulate and dissolved organic carbon in runoff: Entering uncharted waters? *Geophysical Research Letters*, 40(7), 1322–1327. <https://doi.org/10.1002/grl.50306>

Drake, T. W., Raymond, P. A., & Spencer, R. G. M. (2018). Terrestrial carbon inputs to inland waters: A current synthesis of estimates and uncertainty. *Limnology and Oceanography Letters*, 3(3), 132–142. <https://doi.org/10.1002/lol2.10055>

Dusek, J., Vogel, T., Dohnal, M., Barth, J. A. C., Sanda, M., Marx, A., & Jankovec, J. (2017). Dynamics of dissolved organic carbon in hillslope discharge: Modeling and challenges. *Journal of Hydrology*, 546, 309–325. <https://doi.org/10.1016/j.jhydrol.2016.12.054>

Duval, T. P. (2019). Rainfall partitioning through a mixed cedar swamp and associated C and N fluxes in Southern Ontario, Canada. *Hydrological Processes*, 33(11), 1510–1524. <https://doi.org/10.1002/hyp.13414>

Duvaneck, M. J., Thompson, J. R., Gustafson, E. J., Liang, Y., & de Brujin, A. M. G. (2016). Recovery dynamics and climate change effects to future New England forests. *Landscape Ecology*, 32(7), 1385–1397. <https://doi.org/10.1007/s10980-016-0415-5>

Feng, D., Beighley, E., Hughes, R., & Kimbro, D. (2016). Spatial and temporal variations in eastern U.S. hydrology: Responses to global climate variability. *JAWRA Journal of the American Water Resources Association*, 52(5), 1089–1108. <https://doi.org/10.1111/1752-1688.12445>

Germer, S., Neill, C., Krusche, A. V., Neto, S. C. G., & Elsenbeer, H. (2007). Seasonal and within-event dynamics of rainfall and throughfall chemistry in an open tropical rainforest in Rondônia, Brazil. *Biogeochemistry*, 86(2), 155–174. <https://doi.org/10.1007/s10533-007-9152-9>

Germer, S., Zimmermann, A., Neill, C., Krusche, A. V., & Elsenbeer, H. (2012). Disproportionate single-species contribution to canopy-soil nutrient flux in an Amazonian rainforest. *Forest Ecology and Management*, 267, 40–49. <https://doi.org/10.1016/j.foreco.2011.11.041>

Hansen, K., Draaijers, G., Ivens, W., Gundersen, P., & Van Leeuwen, N. (1994). Concentration variations in rain and canopy throughfall collected sequentially during individual rain events. *Atmospheric Environment*, 28(20), 3195–3205. [https://doi.org/10.1016/1352-2310\(94\)00176-1](https://doi.org/10.1016/1352-2310(94)00176-1)

Hernes, P. J., Spencer, R. G. M., Dyda, R. Y., O'Geen, A. T., & Dahlgren, R. A. (2017). The genesis and exodus of vascular plant DOM from an oak woodland landscape. *Frontiers in Earth Science*, 5. <https://doi.org/10.3389/feart.2017.00009>

Hornberger, G. M., Bencala, K. E., & McKnight, D. M. (1994). Hydrological controls on dissolved organic carbon during snowmelt in the Snake River near Montezuma, Colorado. *Biogeochemistry*, 25(3), 147–165. <https://doi.org/10.1007/bf00024390>

Howard, D., Stan, J., Whitetree, A., Zhu, L., & Stubbins, A. (2018). Interstorm Variability in the biolability of tree-derived dissolved organic matter (Tree-DOM) in throughfall and stemflow. *Forests*, 9(5), 236. <https://doi.org/10.3390/f9050236>

Huntington, T. G., Richardson, A. D., McGuire, K. J., & Hayhoe, K. (2009). Climate and hydrological changes in the northeastern United States: Recent trends and implications for forested and aquatic ecosystems. *Canadian Journal of Forest Research*, 39(2), 199–212. <https://doi.org/10.1139/x08-116>

Iavorivska, L., Boyer, E. W., & DeWalle, D. R. (2016). Atmospheric deposition of organic carbon via precipitation. *Atmospheric Environment*, 146, 153–163. <https://doi.org/10.1016/j.atmosenv.2016.06.006>

Inamdar, S. P., Dhillon, G., Singh, S., Dutta, S., Levia, D., Scott, D., et al. (2013). Temporal variation in end-member chemistry and its influence on runoff mixing patterns in a forested, Piedmont catchment. *Water Resources Research*, 49(4), 1828–1844. <https://doi.org/10.1002/wrcr.20158>

Inamdar, S. P., & Mitchell, M. J. (2006). Hydrologic and topographic controls on storm-event exports of dissolved organic carbon (DOC) and nitrate across catchment scales. *Water Resources Research*, 42(3), W03421. <https://doi.org/10.1029/2005wr004212>

Inamdar, S. P., & Mitchell, M. J. (2007). Contributions of riparian and hillslope waters to storm runoff across multiple catchments and storm events in a glaciated forested watershed. *Journal of Hydrology*, 341(1–2), 116–130. <https://doi.org/10.1016/j.jhydrol.2007.05.007>

Jansen, B., Kalbitz, K., & McDowell, W. H. (2014). Dissolved organic matter: Linking soils and aquatic systems. *Vadose Zone Journal*, 13(7). <https://doi.org/10.2136/vzj2014.05.0051>

Johnson, M. S., & Lehmann, J. (2016). Double-funneling of trees: Stemflow and root-induced preferential flow. *Écoscience*, 13(3), 324–333. <https://doi.org/10.2980/1195-6860-13-3-324.1>

Johnson, M. S., Lehmann, J., Selva, E. C., Abdo, M., Riha, S., & Couto, E. G. (2006). Organic carbon fluxes within and streamwater exports from headwater catchments in the southern Amazon. *Hydrological Processes*, 20(12), 2599–2614. <https://doi.org/10.1002/hyp.6218>

Kassambara, A. (2020). Package ‘rstatix’, edited, pp. Pipe-friendly framework for basic statistical tests.

Klotzbücher, T., Kaiser, K., & Kalbitz, K. (2014). Response of dissolved organic matter in the forest floor of a temperate spruce stand to increasing throughfall. *Vadose Zone Journal*, 13(7). <https://doi.org/10.2136/vzj2013.10.0180>

Kreyling, J. (2020). The ecological importance of winter in temperate, boreal, and arctic ecosystems in times of climate change. In Cánovas, F. M., Lütge, U., Leuschner, C., & Risueño, M.-C. (Eds.), *Progress in botany* (Vol. 81, pp. 377–399). Cham: Springer International Publishing. [https://doi.org/10.1007/124\\_2019\\_35](https://doi.org/10.1007/124_2019_35)

Kristensen, H. L., Gundersen, P., Callesen, I., & Reinds, G. J. (2004). Throughfall nitrogen deposition has different impacts on soil solution nitrate concentration in European coniferous and deciduous forests. *Ecosystems*, 7(2). <https://doi.org/10.1007/s10021-003-0216-y>

Laudon, H., Tetzlaff, D., Soulsby, C., Carey, S., Seibert, J., Buttle, J., et al. (2013). Change in winter climate will affect dissolved organic carbon and water fluxes in mid-to-high latitude catchments. *Hydrological Processes*, 27(5), 700–709. <https://doi.org/10.1002/hyp.9686>

Leonard, R. E (1961). Interception of Precipitation by Northern Hardwoods. (Vol. 16). PA, Upper Darby: U.S. Department of Agriculture, Northeastern Forest Experiment Station.

Levia, D. F. (2003). Winter stemflow leaching of nutrient-ions from deciduous canopy trees in relation to meteorological conditions. *Agricultural and Forest Meteorology*, 117(1–2), 39–51. [https://doi.org/10.1016/s0168-1923\(03\)00040-6](https://doi.org/10.1016/s0168-1923(03)00040-6)

Levia, D. F., & Frost, E. E. (2006). Variability of throughfall volume and solute inputs in wooded ecosystems. *Progress in Physical Geography: Earth and Environment*, 30(5), 605–632. <https://doi.org/10.1177/0309133306071145>

Levia, D. F., & Germer, S. (2015). A review of stemflow generation dynamics and stemflow–environment interactions in forests and shrublands. *Reviews of Geophysics*, 53(3), 673–714. <https://doi.org/10.1002/2015rg000479>

Levia, D. F., & Herwitz, S. R. (2005). Interspecific variation of bark water storage capacity of three deciduous tree species in relation to stemflow yield and solute flux to forest soils. *Catena*, 64(1), 117–137. <https://doi.org/10.1016/j.catena.2005.08.001>

Levia, D. F., Van Stan, J. T., Mage, S. M., & Kelley-Hauske, P. W. (2010). Temporal variability of stemflow volume in a beech-yellow poplar forest in relation to tree species and size. *Journal of Hydrology*, 380(1–2), 112–120. <https://doi.org/10.1016/j.jhydrol.2009.10.028>

Manzoni, S., Trofymow, J. A., Jackson, R. B., & Porporato, A. (2010). Stoichiometric controls on carbon, nitrogen, and phosphorus dynamics in decomposing litter. *Ecological Monographs*, 80(1), 89–106. <https://doi.org/10.1890/09-0179.1>

McDowell, W. H., & Likens, G. E. (1988). Origin, composition, and flux of dissolved organic carbon in the Hubbard Brook Valley. *Ecological Monographs*, 58(3), 177–195. <https://doi.org/10.2307/2937024>

McDowell, W. H., Pérez-Rivera, K. X., & Shaw, M. E. (2020). Assessing the ecological significance of throughfall in forest ecosystems. In *Assessing the ecological significance of throughfall in forest ecosystems* (pp. 299–318). Forest-Water Interactions. [https://doi.org/10.1007/978-3-030-26086-6\\_13](https://doi.org/10.1007/978-3-030-26086-6_13)

McDowell, W. H., & Wood, T. (1984). Podzolization: Soil processes control dissolved organic carbon concentrations in stream water. *Soil Science*, 137(1), 23–32. <https://doi.org/10.1097/00010694-198401000-00004>

McGee, G. G., Cardon, M. E., & Kiernan, D. H. (2019). Variation in *Acer saccharum* Marshall (Sugar Maple) bark and stemflow characteristics: Implications for epiphytic bryophyte communities. *Northeastern Naturalist*, 26(1), 214–235. <https://doi.org/10.1656/045.026.0118>

McGlynn, B. L., McDonnell, J. J., Seibert, J., & Kendall, C. (2004). Scale effects on headwater catchment runoff timing, flow sources, and groundwater-streamflow relations. *Water Resources Research*, 40(7), W07504. <https://doi.org/10.1029/2003wr002494>

Meyer, J. L., & Tate, C. M. (1983). The effects of watershed disturbance on dissolved organic carbon dynamics of a stream. *Ecology*, 64(1), 33–44. <https://doi.org/10.2307/1937326>

Michalzik, B., Kalbitz, K., Park, J. H., Solinger, S., & Matzner, E. (2001). Fluxes and concentrations of dissolved organic carbon and nitrogen: A synthesis for temperate forests. *Biogeochemistry*, 52(2), 173–205. <https://doi.org/10.1023/a:1006441620810>

Michalzik, B., & Stadler, B. (2005). Importance of canopy herbivores to dissolved and particulate organic matter fluxes to the forest floor. *Geoderma*, 127(3–4), 227–236. <https://doi.org/10.1016/j.geoderma.2004.12.006>

Moatar, F., Abbott, B. W., Minaudo, C., Curie, F., & Pinay, G. (2017). Elemental properties, hydrology, and biology interact to shape concentration–discharge curves for carbon, nutrients, sediment, and major ions. *Water Resources Research*, 53(2), 1270–1287. <https://doi.org/10.1002/2016wr019635>

Mulholland, P. J. (2002). Large-Scale patterns in dissolved organic carbon concentration, flux, and sources. In Findlay, S., & Sinsabaugh, R. L. (Eds.), *Aquatic ecosystems: Interactivity of dissolved organic matter* (pp. 139–160). Burlington, USA: Elsevier Science & Technology.

Murdoch, P. S., Baron, J. S., & Miller, T. L. (2000). Potential effects of climate change on surface-water quality in North America. *JAWRA Journal of the American Water Resources Association*, 36(2), 347–366. <https://doi.org/10.1111/j.1752-1688.2000.tb04273.x>

Nayak, A., Chandler, D. G., Marks, D., McNamara, J. P., & Seyfried, M. (2008). Correction of electronic record for weighing bucket precipitation gauge measurements. *Water Resources Research*, 44(4), W00D11. <https://doi.org/10.1029/2008wr006875>

Neff, J. C., & Asner, G. P. (2001). Dissolved organic carbon in terrestrial ecosystems: Synthesis and a model. *Ecosystems*, 4(1), 29–48. <https://doi.org/10.1007/s100210000058>

Neu, V., Ward, N. D., Krusche, A. V., & Neill, C. (2016). Dissolved organic and inorganic carbon flow paths in an Amazonian transitional forest. *Frontiers in Marine Science*, 3. <https://doi.org/10.3389/fmars.2016.00114>

Ouimette, A. P., Ollinger, S. V., Richardson, A. D., Hollinger, D. Y., Keenan, T. F., Lepine, L. C., & Vadeboncoeur, M. A. (2018). Carbon fluxes and interannual drivers in a temperate forest ecosystem assessed through comparison of top-down and bottom-up approaches. *Agricultural and Forest Meteorology*, 256–257, 420–430. <https://doi.org/10.1016/j.agrformet.2018.03.017>

Park, B. B., Yanai, R. D., Fahey, T. J., Bailey, S. W., Siccama, T. G., Shanley, J. B., & Cleavitt, N. L. (2008). Fine root dynamics and forest production across a calcium gradient in northern hardwood and conifer ecosystems. *Ecosystems*, 11, 325–341. <https://doi.org/10.1007/s10021-008-9126-3>

Parr, D., & Wang, G. (2014). Hydrological changes in the U.S. Northeast using the Connecticut River Basin as a case study: Part 1. Modeling and analysis of the past. *Global and Planetary Change*, 122, 208–222. <https://doi.org/10.1016/j.gloplacha.2014.08.009>

Perdrial, J., Brooks, P. D., Swetnam, T., Lohse, K. A., Rasmussen, C., Litvak, M., et al. (2018). A net ecosystem carbon budget for snow dominated forested headwater catchments: Linking water and carbon fluxes to critical zone carbon storage. *Biogeochemistry*, 138(3), 225–243. <https://doi.org/10.1007/s10533-018-0440-3>

Ponette-González, A. G., Van Stan, J. T., & Magyar, D. (2020). Things seen and unseen in throughfall and stemflow. In *Precipitation partitioning by vegetation* (pp. 71–88). Springer. [https://doi.org/10.1007/978-3-030-29702-2\\_5](https://doi.org/10.1007/978-3-030-29702-2_5)

Qualls, R. G. (2020). Role of precipitation partitioning in litter biogeochemistry. In *Precipitation partitioning by vegetation* (pp. 163–182). Springer. [https://doi.org/10.1007/978-3-030-29702-2\\_11](https://doi.org/10.1007/978-3-030-29702-2_11)

Qualls, R. G., & Haines, B. L. (1992). Biodegradability of dissolved organic matter in forest throughfall, soil solution, and stream water. *Soil Science Society of America Journal*, 56(2), 578–586. <https://doi.org/10.2136/sssaj1992.03615995005600020038x>

Qualls, R. G., Haines, B. L., & Swank, W. T. (1991). Fluxes of dissolved organic nutrients and humic substances in a deciduous forest. *Ecology*, 72(1), 254–266. <https://doi.org/10.2307/1938919>

Raymond, P. A., & Saiers, J. E. (2010). Event controlled DOC export from forested watersheds. *Biogeochemistry*, 100(1–3), 197–209. <https://doi.org/10.1007/s10533-010-9416-7>

Raymond, P. A., Saiers, J. E., & Sobczak, W. V. (2016). Hydrological and biogeochemical controls on watershed dissolved organic matter transport: Pulse-shunt concept. *Ecology*, 97(1), 5–16. <https://doi.org/10.1890/14-1684.1>

Rosier, C. L., Levia, D. F., Van Stan, J. T., Aufdenkampe, A., & Kan, J. (2016). Seasonal dynamics of the soil microbial community structure within the proximal area of tree boles: Possible influence of stemflow. *European Journal of Soil Biology*, 73, 108–118. <https://doi.org/10.1016/j.ejsobi.2016.02.003>

Runkel, R. L., Crawford, C. G., & Cohn, T. A. (2004). Load Estimator (LOADEST): A FORTRAN program for estimating constituent loads in streams and rivers. In *U.S. Geological survey techniques and methods book 4*. USGS. <https://doi.org/10.3133/tm4a5>

Runkel, R. L., & De Cicco, L. (2017). *rloadest: River load estimation*. R package version 0.4.5.

Ryan, K. A., Shanley, J., Adler, T., Chalmers, A., Perdrial, J., & Stubbins, A. (2021). *Storm event dissolved organic carbon and total dissolved nitrogen concentrations and yields for precipitation, throughfall, stemflow and stream water and hourly streamflow and precipitation record for the W-9 catchment, Sleepers River research watershed, 2017 and 2018*. U.S. Geological Survey data release. <https://doi.org/10.5066/P9OCS8P7>

Sadeghi, S. M. M., Gordon, D. A., & Van Stan, J. T., II (2020). A global synthesis of throughfall and stemflow hydrometeorology. In Van Stan, J. T. II, Gutmann, E., & Friesen, J. (Eds.), *Precipitation partitioning by vegetation: A global synthesis* (pp. 49–70). Cham: Springer International Publishing. [https://doi.org/10.1007/978-3-030-29702-2\\_4](https://doi.org/10.1007/978-3-030-29702-2_4)

Saunders, T. J., McClain, M. E., & Llerena, C. A. (2006). The biogeochemistry of dissolved nitrogen, phosphorus, and organic carbon along terrestrial-aquatic flowpaths of a montane headwater catchment in the Peruvian Amazon. *Hydrological Processes*, 20(12), 2549–2562. <https://doi.org/10.1002/hyp.6215>

Sebestyen, S. D., Boyer, E. W., & Shanley, J. B. (2009). Responses of stream nitrate and DOC loadings to hydrological forcing and climate change in an upland forest of the northeastern United States. *Journal of Geophysical Research: Biogeosciences*, 114(G2), G02002. <https://doi.org/10.1029/2008jg000778>

Sebestyen, S. D., Boyer, E. W., Shanley, J. B., Kendall, C., Doctor, D. H., Aiken, G. R., & Ohte, N. (2008). Sources, transformations, and hydrological processes that control stream nitrate and dissolved organic matter concentrations during snowmelt in an upland forest. *Water Resources Research*, 44(12), W12410. <https://doi.org/10.1029/2008wr006983>

Sebestyen, S. D., Ross, D. S., Shanley, J. B., Elliott, E. M., Kendall, C., Campbell, J. L., et al. (2019). Unprocessed atmospheric nitrate in waters of the northern forest region in the U.S. and Canada. *Environmental Science & Technology*, 53(7), 3620–3633. <https://doi.org/10.1021/acs.est.9b01276>

Sebestyen, S. D., Shanley, J. B., Boyer, E. W., Kendall, C., & Doctor, D. H. (2014). Coupled hydrological and biogeochemical processes controlling variability of nitrogen species in streamflow during autumn in an upland forest. *Water Resources Research*, 50(2), 1569–1591. <https://doi.org/10.1002/2013wr013670>

Shanley, J. B. (2000). *Sleepers River, Vermont: A water, energy, and biogeochemical budgets program site*. (pp. 166–99). US Geological Survey. Fact Sheet. <https://doi.org/10.3133/fs16699>

Shanley, J. B., Kendall, C., Smith, T. E., Wolock, D. M., & McDonnell, J. J. (2002). Controls on old and new water contributions to stream flow at some nested catchments in Vermont, USA. *Hydrological Processes*, 16(3), 589–609. <https://doi.org/10.1002/hyp.312>

Shanley, J. B., Krám, P., Hruška, J., & Bullen, T. D. (2004). A biogeochemical comparison of two well-buffered catchments with contrasting histories of acid deposition. *Water, Air, & Soil Pollution: Focus*, 4(2/3), 325–342. <https://doi.org/10.1023/B:WAFO.0000028363.48348.a4>

Shanley, J. B., Sebestyen, S. D., McDonnell, J. J., McGlynn, B. L., & Dunne, T. (2015). Water's Way at Sleepers River watershed – Revisiting flow generation in a post-glacial landscape, Vermont, USA. *Hydrological Processes*, 29(16), 3447–3459. <https://doi.org/10.1002/hyp.10377>

Siebert, C. M., Levia, D. F., Leathers, D. J., Van Stan, J. T., & Mitchell, M. J. (2017). Do storm synoptic patterns affect biogeochemical fluxes from temperate deciduous forest canopies? *Biogeochemistry*, 132(3), 273–292. <https://doi.org/10.1007/s10533-017-0300-6>

Sipler, R. E., & Bronk, D. A. (2015). Dynamics of dissolved organic nitrogen. In Hansell, D., & Carlson, C. (Eds.), *Biogeochemistry of marine dissolved organic matter* (pp. 127–232). <https://doi.org/10.1016/b978-0-12-405940-5.00003-0>

Spiess, A.-N. (2018). Package ‘propagate’, edited, pp. Propagation of uncertainty using higher-order Taylor expansion and Monte Carlo simulation.

Springston, G. E., & Haselton, G. M. (1999). *Surficial geologic map of the eastern portion of the st. Johnsbury quadrangle*. Survey, V. G. (Ed.). Vermont.

Stubbins, A., Guillemette, F., & Van Stan, J. T., II (2020). Throughfall and stemflow: The crowning headwaters of the aquatic carbon cycle. In *Precipitation partitioning by vegetation* (pp. 121–132). [https://doi.org/10.1007/978-3-030-29702-2\\_8](https://doi.org/10.1007/978-3-030-29702-2_8)

Stubbins, A., Silva, L. M., Dittmar, T., & Van Stan, J. T. (2017). Molecular and optical properties of tree-derived dissolved organic matter in throughfall and stemflow from live oaks and eastern red cedar. *Frontiers in Earth Science*, 5. <https://doi.org/10.3389/feart.2017.00022>

Tang, G., Beckage, B., Smith, B., & Miller, P. A. (2010). Estimating potential forest NPP, biomass and their climatic sensitivity in New England using a dynamic ecosystem model. *Ecosphere*, 1(6), 18. <https://doi.org/10.1890/es10-00087.1>

Tank, S. E., Fellman, J. B., Hood, E., & Kritzberg, E. S. (2018). Beyond respiration: Controls on lateral carbon fluxes across the terrestrial-aquatic interface. *Limnology and Oceanography Letters*, 3(3), 76–88. <https://doi.org/10.1002/lol2.10065>

Tetzlaff, D., Buttle, J., Carey, S. K., McGuire, K., Laudon, H., & Soulsby, C. (2015). Tracer-based assessment of flow paths, storage and runoff generation in northern catchments: A review. *Hydrological Processes*, 29(16), 3475–3490. <https://doi.org/10.1002/hyp.10412>

Todorov, V., & Filzmoser, P. (2009). An object-oriented framework for robust multivariate analysis. *Journal of Statistical Software*, 32(3). <https://doi.org/10.18637/jss.v032.i03>

Trenberth, K. E. (2011). Changes in precipitation with climate change. *Climate Research*, 47(1), 123–138. <https://doi.org/10.3354/cr00953>

Van Gaelen, N., Verheyen, D., Ronchi, B., Struyf, E., Govers, G., Vanderborght, J., & Diels, J. (2014). Identifying the transport pathways of dissolved organic carbon in contrasting catchments. *Vadose Zone Journal*, 13(7). <https://doi.org/10.2136/vzj2013.11.0199>

Van Stan, J. T., & Gordon, D. A. (2018). Mini-review: Stemflow as a resource limitation to near-stem soils. *Frontiers in Plant Science*, 9, 248. <https://doi.org/10.3389/fpls.2018.000248>

Van Stan, J. T., & Stubbins, A. (2018). Tree-DOM: Dissolved organic matter in throughfall and stemflow. *Limnology and Oceanography Letters*, 3(3), 199–214. <https://doi.org/10.1002/lol2.10059>

Van Stan, J. T., Wagner, S., Guillemette, F., Whitetree, A., Lewis, J., Silva, L., & Stubbins, A. (2017). Temporal dynamics in the concentration, flux, and optical properties of tree-derived dissolved organic matter in an epiphyte-laden oak-cedar forest. *Journal of Geophysical Research: Biogeosciences*, 122(11), 2982–2997. <https://doi.org/10.1002/2017jg004111>

Vaughan, M. C. H., Bowden, W. B., Shanley, J. B., Vermilyea, A., Sleeper, R., Gold, A. J., et al. (2017). High-frequency dissolved organic carbon and nitrate measurements reveal differences in storm hysteresis and loading in relation to land cover and seasonality. *Water Resources Research*, 53(7), 5345–5363. <https://doi.org/10.1002/2017wr020491>

Webster, J. R., & Meyer, J. L. (1997). Organic Matter Budgets for Streams: A Synthesis. *Journal of the North American Benthological Society*, 16(1), 141–161. <https://doi.org/10.2307/1468247>

Wilcke, W., Velescu, A., Leimer, S., Blotevogel, S., Alvarez, P., & Valarezo, C. (2020). Total organic carbon concentrations in ecosystem solutions of a remote tropical montane forest respond to global environmental change. *Global Change Biology*, 26(12), 6989–7005. <https://doi.org/10.1111/gcb.15351>

Yoon, B., & Raymond, P. A. (2012). Dissolved organic matter export from a forested watershed during Hurricane Irene. *Geophysical Research Letters*, 39(18), L18402. <https://doi.org/10.1029/2012gl052785>

You, Y., Xiang, W., Ouyang, S., Zhao, Z., Chen, L., Zeng, Y., et al. (2020). Hydrological fluxes of dissolved organic carbon and total dissolved nitrogen in subtropical forests at three restoration stages in southern China. *Journal of Hydrology*, 583, 124656. <https://doi.org/10.1016/j.jhydrol.2020.124656>

Zimmer, M. A., & McGlynn, B. L. (2018). Lateral, Vertical, and longitudinal source area connectivity drive runoff and carbon export across watershed scales. *Water Resources Research*, 54(3), 1576–1598. <https://doi.org/10.1002/2017wr021718>

Zwanzig, M., Schlicht, R., Frischbier, N., & Berger, U. (2020). Primary steps in analyzing data: Tasks and tools for a systematic data exploration. In *Primary steps in analyzing data: Tasks and tools for a systematic data exploration* (pp. 147–174). Forest-Water Interactions. [https://doi.org/10.1007/978-3-030-26086-6\\_7](https://doi.org/10.1007/978-3-030-26086-6_7)

## References From the Supporting Information

Appling, A. P., Leon, M. C., & McDowell, W. H. (2015). Reducing bias and quantifying uncertainty in watershed flux estimates: The R package loadflex. *Ecosphere*, 6(12), 269. <https://doi.org/10.1890/es14-00517.1>

Aulenbach, B. T., Burns, D. A., Shanley, J. B., Yanai, R. D., Bae, K., Wild, A. D., et al. (2016). Approaches to stream solute load estimation for solutes with varying dynamics from five diverse small watersheds. *Ecosphere*, 7(6). <https://doi.org/10.1002/ecs2.1298>

DeCicco, L., & Oliver, S. (2014). *R package 'rainmaker'*. USGS-R.

R Core Team. (2020). *R: A language and environment for statistical computing*, edited, R Foundation for Statistical Computing. Vienna, Austria.

Runkel, R. L., & De Cicco, L. (2017). *rloadest: River load estimation*. R package version 0.4.5.

Sloto, R. A., & Crouse, M. Y. (1996). *HYSEP: A computer program for streamflow hydrograph separation and analysis*. (Report Rep. 96-4040). (p. 46). Reston, VA. USGS. <https://doi.org/10.3133/wri964040>